Linking onshore-offshore basement rock architecture and brittle faults on the submerged strandflat along the SW Barents Sea Margin; using high-resolution (5x5m) bathymetry data

Kjetil Indrevær[1,2,*] & Steffen G. Bergh[1]

1) Department of Geology, University of Tromsø, N-9037 Tromsø, Norway
2) DONG E&P Norge AS, Roald Amundsens Plass 1, N-9257 Tromsø, Norway

* Corresponding author (e-mail: kjetil@indrevar.no)

Abstract: High-resolution bathymetry data reveal astonishingly detailed and complex morphology on the shallow offshore shelf (strandflat) along the SW Barents Sea Margin, outboard Troms, northern Norway. The features are compared with, and interpreted based on, known onshore geology, including Precambrian basement structures of the West Troms Basement Complex, Caledonian thrust nappes and post-Caledonian passive margin brittle structures. The study reveals that Precambrian basement structures commonly observed onshore, such as a generally steep gneiss foliation, steeply plunging tight to isoclinal intrafolial folds, upright macro-fold limbs, duplexes and high-strain ductile shear zones are also present on the strandflat, including possible offshore continuations of Precambrian meta-supracrustal belts. The results suggest that the strandflat outboard Troms is largely comprised of rocks of West Troms Basement Complex affinity. A contact with Caledonian thrust nappes is interpreted to trend NW-SE within a sound in the northern parts of the study area, where it overlaps with the Late Palaeozoic-Mesozoic Fugløya transfer zone, a possible reactivated portion of a Proterozoic-Palaeozoic basement-seated fault complex. A set of linear NNE-SSW to ENE-WSW trending trenches truncate the ductile fabrics and are interpreted as post-Caledonian brittle faults that formed due to multiple rifting events in the Late Palaeozoic-Mesozoic as parts of the evolution of the passive continental margin of the SW Barents Sea. Aspect analysis reveals a strong correlation between the present day landscape and tectonic elements, which indicate a pervasive tectonic influence on the present day coastal landscape of western Troms and the outboard strandflat.

Introduction

The shallow coastal portion off the coast off northern Norway comprises a distinct morphological phenomenon, the strandflat (e.g. Reusch, 1894; Nansen, 1922; Dahl, 1947; Larsen & Holtedahl, 1985; Corner, 2005; Thorsnes et al., 2009). The strandflat is typically manifested as a horizontal to gently dipping, low-relief surface comprised of exposed basement rocks. In Troms, the strandflat is largely submerged but may potentially, due to its location, be a very important source of information for onshore-offshore correlation studies. Any minor relief such as scarps, gullies, trenches, slopes, ridges, etc. visible on data covering the submerged strandflat may be the product of tectonic processes, such as foliation, folds, shear zones, faults and cleavages, (cf. Thorstensen, 2011) and thus give valuable insight into the margin architecture.

In recent years, the Norwegian government has as a part of the MAREANO project collected high-resolution (5x5m) bathymetry data along the coast of Norway. The data is partly available online (mareano.no) and has been widely used within geological sciences to for example map and resolve the glaciation and deglaciation history of the Norwegian shelf or to study submarine canyons and evidence for mass movement (e.g. Ottesen et al., 2005; Rydningen et al., 2013; Rise et al., 2013). For tectonic onshore-offshore studies, however, examples using bathymetry data as a correlation tool are farther apart. This is mainly due to the military restrictions on the data, which limits the resolution to only 50x50m within 12 nautical miles of the coast. This includes more or less all of the submerged strandflat along the Norwegian coast, leaving any detailed study of the strandflat difficult.

However, for the purpose of this study we have been granted access to, and permission to publish, high-resolution (5x5m) MAREANO data within 12 nautical miles of the coast, covering the strandflat offshore Troms (Fig. 1). The dataset is astonishingly rich in detail and may likely be used to solve many very different scientific problems. In this study, however, we will solely focus within a tectonic framework, using the data as a tool in the ongoing onshore-offshore correlation project in Troms and western Finnmark (Gagama, 2005; Eig, 2008; Hansen, 2009; Thorstensen, 2011; Indrevær et al., 2013; 2014). We aim to interpret and explain the strandflat morphology on the basis of known onshore ductile basement fabrics and brittle fault trends. The study aims to improve the understanding of the onshore and offshore SW Barents Sea margin architecture, including (i) the lateral offshore extension of the West Troms Basement Complex (WTBC), (ii) the offshore distribution of Caledonian thrust nappes and (iii) the distribution and linkage of Late Palaeozoic-Mesozoic brittle fault zones and how they relate to onshore fault complexes, such as the Vestfjorden-Vanna Fault Complex (VVFC, e.g. Olesen et al., 1997) and offshore fault complexes, such as the Troms-Finnmark Fault Complex (TFFC, e.g. Gabrielsen et al., 1990).

Geological Setting

In order to interpret morpho-tectonic elements on the strandflat with confidence, it is crucial to have a good understanding of the onshore geology. In the following, a description of the main bedrock lithologies, the ductile and brittle fabrics onshore and the different models proposed for the formation of the strandflat is given.

Precambrian structures of the West Troms Basement Complex

The outer islands of Troms constitute a major basement horst, the West Troms Basement Complex (Fig. 1). The horst is made up of a range of Meso- and Neoarchaean (2.9-2.6 Ga) tonalitic, trondhjemitic and anorthositic gneisses (TTG-gneisses), metasupracrustal belts (2.85-1.9 Ga), and felsic, mafic and ultramafic igneous rocks (2.4-1.75 Ga) (Corfu et al., 2003; Bergh et al., 2010; Myhre et al., 2011, 2013). The ductile deformation is the result of a complex tectonic history in the region, covering a large time span (Bergh et al., 2010): The host-rocks of the TTG-gneisses were igneous tonalites metamorphosed and deformed during a Neoarchean orogenic event (2.69-2.56 Ga; Myhre et al., 2013), producing a main N-S striking gneiss foliation with variable dip, intrafolial ductile shear zones and tight folds (Bergh et al., 2010). This event was followed by crustal extension and mafic dyke intrusions (2.40 Ga). The main architecture of the TTG-gneisses and metasupracrustal belts was the result of a major orogenic event, the Svecofennian, in the Palaeoproterozoic (1.9-1.75 Ga), which included (Fig. 2): (i) tight to isoclinal, NW-SE trending folds with moderate plunges and SW-dipping mylonitic ductile shear zones formed by NE-SW crustal shortening (D1-event), (ii) regional NW-SE trending, open to tight upright folding of the mylonitic foliation (D2-event), (iii) steeply N-plunging sinistral shear folds and associated, steep conjugate NNW-SSE and NW-SE trending ductile strike-shear zones of regional significance (D3-event) and (iv) NE-SW trending upright folds, SE-directed ductile thrust faults and NE-SW and ESE-WNW trending semi-ductile strike-slip shear zones that formed synchronoulys, but orogen-parallel relative to the D3 event in the northern part of the WTBC.

The metasupracrustal belts consist of various meta-conglomerates, meta-psammites, mica-schists and mafic to intermediate meta-volcanic rocks (Zwaan, 1989; Pedersen, 1997; Motuza et al., 2001). They dominantly trend NW-SE and some may be traced for 10's of kilometers along strike, while others define folded, discontinuous inliers or dismembered enclaves that obliquely truncate the Neoarchean foliation in the surrounding gneisses (Bergh et al., 2010). The Svecofennian deformation of the meta-supracrustal belts produced similar structures in the adjacent TTG-gneisses (cf. Armitage & Bergh 2005).

The Senja Shear Belt (Zwaan, 1995; Bergh et al., 2010) defines a network of such metasupracrustal belts thought to be a Palaeoproterozoic terrane boundary. This more than 30 km wide shear belt is delimited from the surrounding TTG-gneisses by the Svanfjellet metasupracrustal belt in the southwest and the Torsnes meta-supracrustal belt in the northeast

(Fig. 3). Internally, several separated meta-supracrustal belts and inliers, including the Astridal and Nøringen belt, are sandwiched between granitic and mafic TTG-gneisses. The width of the belts varies along strike, and anastomosing and lens-shaped ductile shear zones can be traced into the surrounding gneisses. The dominant fabric of the Astridal belt is a mylonitic foliation formed axial-planar to isoclinal folds (D1), which is macrofolded into upright antiforms and synforms (D2), and later folded by steeply plunging mostly sinistral drag folds (D3) (Fig. 3: Bergh et al., 2010). Shear zones along the Astridal belt contacts to neighboring granitic gneisses define macroscale, sinistral duplexes that are affected by a steeply plunging sinistral macrofold in the north at Baltsfjorden (Fig. 3). The Astridal belt can be traced from Baltsfjorden along the coastline towards Nøringen (Figs. 3 & 4), where narrow bands of meta-volcanic and meta-psammitic rocks and intercalated ultramafic lenses dominate (Pedersen, 1997). Internally, the ultra-mafic lenses define sinistral duplexes and comprise multiple and cross-cutting smaller ductile shear zones, both sinistral and dextral types (Fig. 4). The Torsnes belt on Kvaløya (Figs. 3) trends NW-SE and is folded into a macroscale, upright syncline (D2) and affected by subvertical folds and sinistral strike-slip shear zones (D3). The N-S trending foliation of the adjacent TTG-gneisses is notably bent into parallelism with the Torsnes belt. An associated sub-vertical macrofold (D3) in the neighbouring gneisses is present farther north, on the islands of Sommarøya and Hillesøya (Fig. 3; Thorstensen, 2011).

The overall NW-SE structural trend in the WTBC is largely parallel with the Archaean and Palaeoproterozoic orogenic belts of the Fennoscandian Shield east of the Scandinavian Caledonides, that stretches from Kola through Finland and Sweden into the Bothnian basin of central Sweden (Gaal & Gorbatchev 1987; Hölttä et al., 2008; Lahtinen et al., 2008; Bergh et al., 2014). Despite its position as a basement outlier west of the Caledonides, the younger Caledonian overprint is generally weak within the WTBC, but is possibly manifested as arc-shaped refolding and SE-directed thrust zones (Corfu et al., 2003; Bergh et al., 2010).

Caledonain thrust nappes

In the Palaeozoic, a collision between Laurentia and Baltica led to the accretion of thrust nappes with a distinct tectonostratigraphy comprised of the Lower-, Middle-, Upper- and Uppermost Allochthons and the southeast- and eastwards translation of up to several hundreds of kilometers of these as a part of the Caledonian Orogeny (e.g. Roberts and Gee, 1985; Roberts, 2003). The Caledonian rocks in northern Troms and western Finnmark is characterised by gently NW-dipping, well-foliated thrust nappes and some large-scale folds.

Within the study area, the islands of Nord-Fugløya and Arnøya are comprised of units belonging to the Caledonian Kalak Nappe Complex (Middle Allochthon). The Kalak Nappe Complex on Nord-Fugløya and Arnøya consists mainly of gently NW-dipping garnet-mica schists and marble units (Roberts, 1974).

Post-Caledonian structures

The Late Palaeozoic-Mesozoic rift-related activity on the west Troms margin (Figs. 1 & 5) (Gabrielsen et al., 1990; Davids et al; 2013) is outlined by widespread NNE-SSW and ENE-WSW trending brittle normal faults that constitute at least two major fault complexes, the Vestfjorden-Vanna and the Troms-Finnmark fault complexes (Gabrielsen et al., 1984, 1990, 2002; Olesen et al., 1997; Indrevær et al., 2013) and a subsidiary NW-SE trending transfer fracture system (cf. Indrevær et al., 2013) (Fig. 5). The onshore fault zones can be divided into the Vestfjorden-Vanna Fault Complex (VVFC), which marks the southeastern boundary of the WTBC, down-dropping the Caledonian nappes to the east in the order of 1-3 km (Forslund, 1988; Opheim & Andresen, 1989; Olesen et al., 1997) and a less prevalent, SE-dipping fault system that runs along the outer rim of the islands of the WTBC (Fig. 1) (Antonsdottir, 2006; Thorstensen, 2011; Indrevær et al., 2013) with displacement in the order of 100's of meters or less (Indrevær et al., 2013). Offshore, the Troms-Finnmark Fault Complex is the dominant basin-bounding fault complex and defines the northwestern limit of the WTBC, down-faulting basement rocks from 4-5km depth on the Finnmark Platform to possibly more than ~10km depth in the Harstad Basin (Fig. 2) (cf. Gabrielsen et al., 1984, 1990; Indrevær et al., 2013). The Troms-Finnmark and Vestfjorden-Vanna Fault Complexes (Fig. 5) can be traced for 100's of kilometers along strike along the North-Norwegian margin, linking up major horst-bounding structural elements in the south, such as the Lofoten and Nordland Ridges, with offshore fault complexes in the north, such as the Ringvassøy-Loppa, Nysleppen and Måsøy Fault Complexes (c.f. Gabrielsen et al., 1990; Olesen et al., 1997; Dore et al., 1997, 1999; Indrevær et al., 2013). The margin is segmented along strike by at least two major transfer fault systems, the Senja Shear Zone and the Fugløya transfer zone, the possible continuations of the Proterozoic-Palaeozoic Bothnian-Senja (and Senja Shear Belt) and the Bothnian-Kvænangen fault complexes, respectively (Berthelsen & Marker, 1986; Gaal & Gorbatchev 1987; Olesen et al., 1990; Henkel, 1991; Doré et al., 1997; Olesen et al., 1997; Hölttä et al., 2008; Lahtinen et al., 2008; Indrevær et al., 2013; Bergh et al., 2014).

Geomorphology of the strandflat

The strandflat along the Norwegian coast is manifested as a horizontal to gently dipping, low-relief surface that typically ranges in elevation from about 40 meters below sea level to a maximum of 100 meters above sea level (cf. Corner, 2005). The strandflat is comprised of highly dissected bedrock commonly draped by a thin layer of Holocene sediments. It is present along large portions of the coast, from Stavanger in the south, to Nordkapp in the north and may locally reach 60km in width. The origin of the strandflat has been widely discussed in the literature (e.g. Reusch, 1894; Nansen, 1922; Asklund, 1928; Dahl, 1947; Büdel, 1978; Larsen & Holtedahl, 1985; Olesen et al., 2013). Several models for the its origin has been discussed, including the strandflat represent a surface of pre-Cretaceous age that formed due to tropical weathering (Asklund, 1928; Büdel, 1978; Olesen et al., 2013). There seems, however, to be a common concensus that the strandflat formed from a combination of frost weathering, sea-ice erosion and marine abrasion during the Quaternary (Reusch, 1894; Nansen, 1922; Dahl, 1947; Larsen & Holtedahl, 1985), likely re-excavating the pre-Cretaceous etch plain by the removal of easily erodable weathered bedrock (cf. Olesen et al., 2013).

In western Troms and Finnmark, the strandflat is at present mainly a submarine feature, varying in width from 2km, outboard northern parts of Senja, up to 30 km north of Nord-Fugløya (Fig. 1). The strandflat is delimited in the east by the high relief, alpine landscape of the outer islands of Troms, with topography reaching >1000 m above sea level. The western limit of the strandflat is defined by abrupt, steeper slopes that separate the strandflat from the bankflat area, which defines the continental shelf from the strandflat towards the continental break (Corner, 2005). The bankflat outboard Troms is characterised by thick glacigenic deposits forming glacially controlled morphology such as troughs and banks (Fig. 1, cf. Rydningen et al., 2013).

Methods and data bases

The 5x5m resolution dataset covers most of the strandflat off the coast of Troms (~4600 km^2), from Senja in the south to Vanna in the north. Minor areas are provided with 25x25m and 50x50m resolution only and a few areas, especially close to shore and in regions with shallow water depths, have no data available at all (Fig. 6). The strandflat outboard Troms seems well suited for a case study like this due to (i) the wide zone of submerged strandflat along this portion of the coast, (ii) the high degree of available high-resolution bathymetry data covering the strandflat, (ii) the relatively well understood onshore basement geology of the outer islands of Troms, including both ductile and brittle deformation features (Zwaan, 1995; Corfu et al., 2003; Bergh et al., 2010; Myhre et al., 2011; Indrevær et al., 2013; 2014) and (iv) the overall margin-perpendicular, NW-SE structural and lithological trends of heterogeneous Precambrian bedrocks (e.g. Bergh et al., 2010), providing an excellent framework for onshore-offshore structural analysis.

The data has been used to produce dip maps, profiles, shadow relief maps (3D-view) and aspect maps in order to highlight morphological features. The aspect maps consider only slopes that dip more than 5°, where the slope direction for each data point is calculated based on the immidiate neighbouring data points (3x3 window). Aerial photographs are used to map and interpret morphology on smaller islands and skerries. Geological maps from NGU and other detailed studies (Pedersen, 1997; Armitage, 2007; Bergh et al., 2010) are used to compare and evaluate features visible on the high-resolution bathymetry data with nearby onshore basement structures.

Results

Regional slope aspect analysis

Aspects for surface slopes dipping more than 5° covering the entire WTBC horst and the outboard subsea strandflat (Fig. 5) shows that the island of Senja is dominated by NE-SW striking slopes, except in its northern portion, where NW-SE trending slopes are common, clearly reflected by the NW-SE trending fjords that spatially overlap with the basement gneiss foliation and the Senja Shear Belt (Figs. 1 & 7). The islands of Kvaløya and Ringvassøya are in general dominated by NNE-SSW to ENE-WSW striking slopes, while the Vanna island is characterised by ~N-S trending larger ridges (Fig. 7). The combined aspect values of all islands within the WTBC reveal that the onshore slope topography is dominated by NW-SE and NE-SW to E-W striking slopes (Fig. 7).

The morphology of the strandflat shows, as expected, a much lower relief and slope variation than onshore topography, with much of the strandflat being characterised by slopes that dip less than 5°. Of steeper slopes, N-S and ENE-WSW striking slopes dominate, including a minor maximum of slopes striking NNW-SSE (Fig. 5). The latter population of slopes are more common outboard the northern portions of Senja and northwest of Nord-Fugløya (Fig. 7).

Comparing onshore and offshore aspect values reveal that slopes of very similar orientations dominate both the bathymetry and the topography, indicating that there are at least some common aspects to the controlling elements of terrain-forming processes on the strandflat and on land.

Morpho-tectonic elements on the strandflat

On a regional scale, the strandflat within the study area is more or less continuous along the outer coast of the WTBC, only interrupted by a few, up to 200m deep, ~E-W trending trenches located at the mouths of sounds and fjords, carved out by glaciers extending from the inland and feeding large glacial ice streams during previous glacial periods (Fig. 1; Vorren et al., 1983; Dahlgren et al., 2005; Rydningen et al., 2013). On a more local scale, the strandflat is dissected by relatively less prevalent trenches that define the outer boundaries of basement blocks and which internally show a lower relief variation, commonly defined by smaller, linear to curved, parallel ridges and truncating trenches.

We describe in detail three areas of the strandflat in western Troms and Finnmark (Fig. 1) that cover key morpho-tectonic elements that may be used to characterise this portion of the SW Barents Sea margin.

Area 1

<u>Local onshore geology</u>

Area 1 (Fig. 8) covers the northwestern parts of Senja and southwestern parts of Kvaløya. Onshore, the geology is dominated by N-S trending, foliated Neoarchaean TTG-gneisses, locally with intercalations of the Ersfjord granite, several NW-SE trending meta-supracrustal belts, including the Astriddal, Nøringen and Torsnes belts and ductile shear zones belonging to the Svecofennian Senja Shear Belt (Figs. 3 & 8; Zwaan, 1995; Bergh et al., 2010).

Post-Caledonian brittle structures within Area 1 include the Bremneset, Tussøya and Hillesøya fault zones (Figs. 3 & 8), which are a part of the SE-dipping fault system that run along the outer rim of the WTBC islands. The Tussøya fault zone (Indrevær et al., 2013, 2014) defines a normal-oblique sinistral fault that dips moderately ESE and separates granitic TTG-gneisses in the footwall from banded mafic and felsic gneisses in the hanging wall. The

Hillesøy fault zone (Fig. 8; Thorstensen, 2011; Indrevær et al., 2013) is comprised of several ENE-dipping faults that merge into subsidiary ENE-dipping fault set. The fault zone is located on the steep northwestern limb of a sub-vertical macrofold on the islands of Sommarøya and Hillesøya (Thorstensen, 2011; Indrevær et al., 2013). Further north, the Bremneset fault zone dips ESE and can be traced along the shore for c. 200 meters, cutting migmatitic TTG-gneisses of the Kattfjord Complex (Fig. 8; Indrevær et al., 2013, 2014).

<u>Morpho-tectonic elements on the strandflat</u>

The strandflat northwest of Nøringen (Fig. 9), is dominated by lens-shaped, flat-topped plateaus and ridges surrounded by anastomosing 25-50 m deep and internally smooth depressions that have a distinct NW-SE trend (Fig. 9a & b). These anastomosing features are well displayed on the aspect map of slope directions in the area (Fig. 9c). E-W trending parallel ridges (red aspect values) to the north truncate and/or curve into parallelism with the anastomosing NW-SE features. A few, more or less developed, NNE-SSW trending, sub-linear trenches (blue aspect values) cut the anastomosing features and curved ridges. Aspect analysis of seabed slopes shown on the map (Fig. 9c) and slope azimuth histograms (Fig. 9d), with dips exceeding 5°, reveals that slopes trending NW-SE dominate the morphology on the seabed.

The strandflat north in Area 1 (Figs. 8 & 10) shows NW-SE trending, linear to curved parallel ridges in the northwest that may be traced for 20 km from the Torsnes Belt in the southeast (Fig. 10). The elongated ridges are typically 1-30m high and 100-500 m wide (Fig. 10a, cross-sections). Northwest of Edøya, these ridges curve into a macroscale z-shaped feature before continuing northwestward. Close to the outer edge of the strandflat, these parallel ridges are obliquely truncated by a E-W trending trench that apparantly displace the morpho-tectonic pattern, thus defining a boundary toward a portion of the strandflat that is characterized by rounded knobs rather than elongated ridges (Fig. 10a & 11a). Outside the zone of parallel ridges, cross-cutting trenches and a chaotic assembly of irregular, often rectangular depressions dominate the strandflat (Fig. 10a). The depressions have variable trends NNE-SSE to ENE-WSW and NW-SE, as illustrated by the aspect map (Fig. 10c). Aspect analysis of slopes with dips > 5° show that slopes trending NW-SE (red and blue aspect values) dominate the seabed morphology within the area (Fig. 10d). Onshore aspects (Fig. 10d; black line) show a larger variation in trends than offshore aspects, which include NE-SW trends, but reveals that slopes striking NW-SE are common onshore as well.

Interpretation

The anastomosing, morpho-tectonic feature visible northwest of Nøringen (Fig. 9) show similar geometry as the sinistral duplexes observed onshore in lenses of foliated granitic gneisses of the Astridal belt (Fig. 3) and ultramafic rocks in meta-supracrustal units of the Nøringen belt (Fig. 4), including an apparent sinistral displacement of the lense along a curved lineament. The anastomosing feature is therefore interpreted as a sinistrally duplexed lens (Fig. 11b). Based on the direct bathymetric link of this feature along the seabed to Nøringen (Fig. 9a), the feature is interpreted to be the offshore continuation of the Palaeoproterozoic Astridal belt, or alternatively a separate meta-supracrustal inlier of the TTG-gneisses, common within the Senja Shear Belt. The outline of this zone on the strandflat is overall similar in trend and width to onshore meta-supracrustal belts, supporting the above interpretation. To the northeast of this zone, distributed elongated ridges and depressions are considered to reflect the exposed TTG-gneiss foliation. The gneiss foliation is transposed and/or tight to isoclinally folded and modified along the contact to the meta-supracrustal belt in a similar manner as observed onshore along the Astridal belt (Fig. 3), suggesting a sinistral sense of shear (Fig. 11b).

The zone of NW-SE trending elongated and parallel ridges north in area 1 (Fig. 10) can be traced directly southeastward into the Torsnes meta-supracrustal belt. Thus, these ridges may represent the offshore continuation of the upright macrofolded (D2) units of the Torsnes belt (Fig. 11c). This linkage is supported by the fact that meta-supracrustal rocks partly step onshore Edøya (Zwaan et al., 1998). Northwest of Edøya (Fig. 11c), the macroscale z-shaped curvature of the belt is interpreted as a sub-vertical macrofold (D3) formed by NW-SE directed, sinistral ductile shearing along the Torsnes belt boundaries. A similar, but more localized Svecofennian ductile shear zone may be present on the northern limb of this macrofold, merging southeastward just east of Hillesøya (Fig. 11c). Close to the strandflat edge, the presumed continuation of the Torsnes belt is truncated by an E-W trending lineament, separating homogenous rocks in the north from the well-foliated rocks in the south (Fig. 11a & c). This lineament is interpreted as either a ductile shear zone that displaced portions of the Torsnes belt, or a lithological, intrusive contact. Granitoid intrusive rocks of both Archean and Svecofennian age, are common within the TTG-gneisses (Andresen, 1980; Corfu et al., 2003), where they truncate ductile Svecofennian fabrics and shear zones (e.g. Bergh et al., 2010). Therefore we suggest this abrupt contact to be lithological and related to some of these intrusions. This inferred granite-gneiss contact may have been tectonically reactivated during e.g. the late Svecofennian deformations events (Bergh et al., 2010), or alternatively during Palaezoic-Mesozoic brittle normal faulting (Indrevær et al., 2013).

Linear and curved, variably trending trenches that truncate many of the curved and parallel ridges must therefore be younger (Fig. 11b & c). In general, these trenches inhabit the same trends as known Late Palaozoic-Mesozoic brittle fault zones onshore (Indrevær et al., 2013). Consequently, the linear trenches are interpreted as fault scarps, partly excavated by strandflat-forming processes. The chaotic array of rectangular to orthogonal depressions (Fig. 11c), with long axes oriented parallel to trends of brittle faults, can tentatively be interpreted as smaller basins delimited by normal faults.

In summary, Area 1 shows morpho-tectonic elements interpreted to be the offshore continuation of two metasupracrustal belts, the Astridal/Nøringen belt and the Torsnes belt. In addition, the inferred ductile structures are truncated by NNE-SSW and ENE-WSW trending trenches that are interpreted as Late Palaeozoic-Mesozoic brittle normal faults.

Area 2:

<u>Local onshore geology</u>

Area 2 covers the strandflat outboard the northern parts of Kvaløya, Ringvassøya and Rebbensøya in the central portion of the WTBC, and includes the smaller islands of Vengsøya, Gjøssøya, Sandøya and Sørfugløya (Fig. 12). The islands of Vengsøya and Gjøssøya are comprised of heterogenous TTG-gneisses and amphibolitic gneisses of the Kattfjord Complex, with intercalations of biotite schists, meta-psammites, quartzites and some meta-volcanic rocks (Grogan & Zwaan, 1997). On Vengsøya, the foliation is in general striking NW-SE and is tightly folded into a steeply plunging (D3) macrofold on the southwestern part of the island (Fig. 12; Grogan & Zwaan, 1997). On Gjøssøya, the foliation strikes NNE-SSW. Granitic intrusions are widespread both as lenses parallel to the foliation and as irregular, truncating bodies and pegmatite veins.

The islands of Ringvassøya and Rebbenesøya in the north are composed of well-foliated TTG-gneisses that have numerous intercalations of amphibolitic gneisses, and commonly cut by irregular granite intrusions (Grogan & Zwaan, 1997). The TTG-gneiss foliation on Rebbenesøya and northern parts of Ringvassøya trend on average N-S, but is bent into a NW-SE orientation in the south, adjacent to a high-strain, migmatitic ductile shear zone presumed to be a Neoarchaean terrane boundary and termed the Kvalsund shear zone (Fig. 12; Myhre et al., 2013).

Farther northwest, on the island of Sandøya, the foliation within quartz-feldspathic biotite gneisses dips steeply toward WNW (Fig. 12, inset map). A ~0.5km wide, foliation-parallel quartzite layer traverses the island on its eastern side (Armitage, 2007; Gjerløv, 2008).

<u>Morpho-tectonic elements on the strandflat</u>

The strandflat just west of Vengsøya and Gjøssøya (Fig. 12), is characterized by a plateau surrounded by narrow, deep trenches (Fig. 13). The plateau shows an internal morphology outlined by parallel elongated ridges that trend NW-SE and curve around in a somewhat complex dome-shaped pattern (Fig. 13a & b). Minor, linear ENE-WSW trending trenches on the plateau truncate the curved parallel ridges. The plateau is delimited in the north by a NE-SW to ENE-WSW trending, ~1km wide, 50 m deep trench and to the south by a c. 2km wide, ~200m deep E-W trending depression that can be traced for ~30km eastward, merging into Skulsfjord on Kvaløya (visible as green and red slopes on the aspect map, Fig. 13c). The elongated ridges on the plateau correspond in attitude with the main TTG-gneiss foliation on the island of Vengsøya (Fig. 12), including the tight isoclinal fold that occurs in the southwestern parts of Vengsøya (also visible from aerial photographs, Fig. 13a). Aspect analysis of slopes with dips exceeding 5° reveals that slopes striking NE-SW and NW-SE (green and red aspect values) dominate the seabed morphology within the area (Fig. 13c & d), which corresponds to the orientation of the large trenches delimiting the plateau.

Within the strait between the islands of Rebbenesøya and Sandøya (Fig. 12), a similar morphological pattern is observed (Fig. 14). The two islands comprise well-foliated TTG-gneisses, with foliation striking mostly N-S, but with opposite dips, i.e. steeply to the east and west, respectively (Fig. 14a & b). Aerial photographs have allowed for interpretative mapping and linkage of the basement foliation surface traces between many smaller islands and skerries (Fig. 14a). The bathymetry data between the two islands reveals a distinct curved ridge that may be traced from the eastern rim of Sandøya northeastward until it curves into a NNW-SSE trend and proceeds southwards to match up with the foliation on Rebbenesøya (Fig. 14a & b). A distinct NNE-SSW trending trench can also clearly be observed east of Sandøya. Aspect analysis reveals that slopes striking N-S to NNE-SSW and WNW-ESE dominate the seabed morphology (Fig. 14c & d, yellow and blue aspect values). The same trends also dominate the onshore topography (Fig. 14d; grey lines).

West of Sandøya, close to the strandflat edge, a >5km wide zone of NNW-trending, parallel ridges is present (Fig. 12, see Figs. 15 & 16 for details). The individual ridges vary from 100-500m in width and 20-75m in height. Within this zone, tightly curved ridges and internally anastomosing wedge-shaped lenses are observed (Fig. 15), enclosed by irregular, aligned depressions (blue and red-yellow aspect values, Fig. 15c & d). Towards the east, the area comprises well-developed parallel ridges separated from a slightly more elevated area. This ridge is mainly covered by 50x50m resolution bathymetry data, but still show less developed lineated morphology. The widespread red to orange and blue aspect values (Fig. 15c & d) reveal that slopes trending N-S to NNW-SSE and NE-SW dominate the seabed morphology in this subarea, which is similar to the main orientation of the zone of parallel ridges. The northern portion of this zone (Fig. 16) shows a network of irregular, variable trending trenches that truncate the parallel ridges such that the strandflat is split up into blocks of distinct geometric characters. Notably, there is a marked east-west change in the elevation of the strandflat across a major escarpment, apparent on the profile (Fig. 16a). This escarpment dips steeply west and displaces the strandflat from less than c. 100 m depth in the east to c. 250 m depth in the west. The escarpment runs northward to link up with the edge of the strandflat (Fig. 16a & b). Aspect analysis reveals that slopes striking NNW-SSE (orange and blue aspect values, Fig. 16c & d) dominate the seabed morphology in this subarea, which reflects the flanks of the NNW-SSE trending ridges visible on the bathymetry data.

The northernmost part of Area 2, northwest of the small island of Sørfugløya (Figs. 12), shows morpho-tectonic elements that are dominated by a set of linear, distinct 200-500m wide steeper slopes trending N-S and NNE-SSW that link up in a system of scarps with a zigzag geometry (Fig. 17a & b). This structure defines an escarpment that separates the inner and outer portions of the strandflat, with c. 200m difference in elevation (Fig. 17a). Weakly developed curved ridges are visible (Fig. 17a). Aspect analysis (Fig. 17c & d) reveals that blue to purple aspect values, corresponding to the NNE-SSW striking escarpments, dominate the seabed morphology in this region, with a minor maximum striking ENE-WSW (green aspect values).

Interpretation

The curved, parallel ridges observed west of Vengsøya and Gjøssøya (Fig. 13) can be directly linked with the basement fabric observed onshore these islands, and thus are interpreted to reflect the bedrock foliation. The dome-shaped and curved nature of ridges on the strandflat suggests that the foliation is folded around a sub-vertical fold axis (D3), making up a tight macrofold with fold limbs trending ~NW-SE (Fig. 18a). This interpretation is supported by similar fold patterns onshore the island of Vengsøya. The minor ENE-WSW trending trenches that truncate the TTG-gneiss foliation, together with the larger and deeper trenches in the north and south of this portion of the strandflat are, based on the similarity in orientations with onshore brittle normal faults (Indrevær et al., 2013), interpreted to represent brittle faults and/or fracture systems.

A similar fold structure (D3) is interpreted to exist in the strait between Sandøya and Rebbenesøya (Fig. 18b). The ridge that continues northward from Sandøya is interpreted to be the continuation of the meta-quartzite unit mapped on Sandøya (Fig. 12, inset map), as a competent unit like quartzite likely would manifests itself as a positive feature on the seabed (Fig. 18b). The ridge curves around and link up with the foliation onshore Rebbenesøya, suggesting that this area represent a major fold hinge with a steeply N-plunging (D3) fold axis. Thus, the fold may explain the opposite dips of foliation onshore Sandøya and Rebbenøya, due to their location on opposite fold limbs.

The wide zone of NNW-SSE trending parallel ridges west of Sandøya (Fig. 12) resemble that of a high-strain ductile shear zone present within TTG-gneisses and meta-supracrustal belts onshore. The internally merging ridges and wedge-shaped lenses within its southern portion (Fig. 19a) are thought to reflect intrafolial tight to isoclinal (D1) macrofolds with transposed shear-lenses, features also commonly identified onshore in Svecofennian ductile shear zones (e.g. Bergh et al., 2010). The orientation of the foliation and hence the contact towards the low-strain zone along the northern portion of the zone is estimated to dip ~35° towards west, based on the asymmetric relief of the ridges (Fig. 16a & b). The shear zone foliation is bent and asymmetrically folded (sinistrally), likely by steep-plunging folds (D3) (Fig. 19a). Importantly, this shear zone may be the strandflat impression of the offshore continuation of the Kvalsund shear zone (Myhre et al., 2013). The abrupt divide from well-foliated ridges against less lineated morphology to the east of this inferred high-strain zone is interpreted to represent a hinge zone of a sub-horizontal, upright NW-SE trending (D2) anticlinal fold (Fig.

19a & b), as is present along the Kvalsund shear zone onshore. Alternatively, this zone may be interpreted as a shear zone or lithologicial boundary against the high-strain shear zone in the west, with e.g. non-migmatized tonalitic gneisses and/or meta-quartzite horizons such as those observed on the island of Sandøya (Armitage, 2007).

The inferred offshore continuation of the Kvalsund shear zone is cut and offset by numerous NNE-SSW to ENE-WSW trending gullies and narrow depressions (Fig. 19a & b). These depressions are interpreted as major brittle faults transecting the entire strandflat in localized zones. The boundary between the high-strain ductile shear zone and an apparently less strained zone to the east (interpreted as a hinge zone) may be dextrally displaced across one such major brittle fault zone in the south of this subarea (Fig. 19b). By assuming pure normal dip-slip displacement along the major brittle fault, a northwards 60° dip of the fault plane and a 35° westward dip of the foliation surface, the apparent 2.2km dextral displacement of the high-strain zone across the fault is calculated to correspond to 1.8km down to the north, normal displacement. Notably, NNE-SSW trending brittle faults are observed to curve into the ENE-WSW trending faults and vica-versa (Fig. 19a).

North in Area 2, an escarpment with zigzag geometry is dominating the seabed morphology (Fig. 20). The zigzag character of the escarpment corresponds with the character of the offshore Troms-Finnmark Fault Complex and the onshore Vestfjorden-Vanna Fault Complex (Gabrielsen et al., 1990; Olesen et al., 1997; Indrevær et al., 2013), and is therefore considered to reflect Late Palaeozoic-Mesozoic brittle normal faults that are defining the western boundary of the strandflat. These presumed faults are well outlined in the cross-sections (Fig. 17a) as a major, overall NW-dipping set of escarpments that vertically offsets the basement surface of the strandflat to a lower elevation and thus allowing for glacigenic sediments to be partly deposited on top (Fig. 20). A set of curved ridges just to the east of the major scarp suggests that the foliation in this area is tightly folded by a N-S trending steeply dipping macrofold (D3).

In summary, the seabed morphology within Area 2 is interpreted to contain at least three D3 macrofolds (Figs. 18 & 20). The folds are associated with the offshore continuation of the Kvalsund shear zone (Figs. 19), which is interpreted to show intrafolial D1-folding (Fig. 19a), and the hinge zone of an upright D2-fold (Fig. 19a, b). The ductile fabrics are cut by numerous inferred Late Palaeozoic-Mesozoic brittle normal faults that truncate the strandflat.

The westernmost scarp of the strandflat is suggested to be connected to Late Palaeozoic-Mesozoic brittle faulting (Fig. 20).

Area 3:

Local onshore geology

Area 3 covers the islands of Vanna and Nord-Fugløya and the strandflat north of these islands (Fig. 21). Vanna is the northernmost island of the exposed West Troms Basement Complex and consists of Neoarchaean tonalitic gneisses that locally are unconformably overlain by the para-autochthonous meta-supracrustal units, the Vanna Group and the Skipsfjord Nappe (Fig. 21; Binns et al., 1980; Johansen 1987; Opheim & Andresen, 1989; Bergh et al., 2007a). The Vanna Group meta-supracrustal unit is also exposed on the island of Spenna, 5 km along strike east of Vanna (Roberts, 1974). In general, the tonalitic gneiss foliation on Vanna is folded by a N-S trending, macroscale, upright antiform plunging southward (Fig. 21). The Skipsfjord nappe is in the north down-faulted by at least 3 km by the SSE-dipping Vannareid-Brurøysund fault zone (Fig. 21), of presumed Mesozoic age (Opheim & Andresen, 1989). This fault zone constitutes a well-defined ENE-WSW trending topographic valley underlain by a >20m wide zone of brittle, cataclastic fault rocks.

The islands of Nord-Fugløya and Arnøya northeast of Vanna (Fig. 21) are both comprised of Palaeozoic, metamorphic Caledonian rocks of the Middle Allochthonous thrust sheets (Roberts, 1974; Ramsay et al., 1985). Dominant rocks are garnet-mica schists and marble units (Roberts 1974) with a foliation on average dipping gently to the NW. The sound between Vanna and the two islands therefore define a prominent regional boundary between the Caledonian thrust nappes to the northeast and the Precambrian rocks of the WTBC to the southwest. Indrevær et al. (2013) considers this sound to be underlain by a major Late Palaozoic-Mesozoic transfer fault zone that formed by reactivation of a Proterozoic-Palaeozoic ductile shear zone (the Bothnian-Kvænangen Fault Complex) (Doré et al., 1997).

Morpho-tectonic elements on the strandflat

The bathymetry data north of Vanna seem to be more influenced by glacial-induced morphology than farther south (Fig. 21). Still, within the western parts of the area, N-S to NNW-SSE trending parallel ridges and gullies are visible (Fig. 22 a & b). In the northern parts, a larger raised portion of the strandflat defines a plateau delimited by a major south-facing escarpment in the south, marked as a green coloured feature on the aspect map (Fig.

22c). The escarpment separates seabed morphology that differs ~ 200m in depth (Figs. 21 & 22a). While the southern, down-dropped part has a diffuse glacial-fill morphology, the plateau itself shows distinct sets of intersecting trenches: the western portion of the plateau comprises smaller E-W, NE-SW and ~N-S trending rhombic bedrock patterns, which are illustrated by blue, red and green values on the aspect map (Fig. 22c). This pattern is abruptly replaced further east on the plateau by a c. 6 km wide zone of ~NNW-SSE trending parallel ridges that run within in a major trough (Fig. 22a & b). East of the N-S trending trough, the rhombic bedrock pattern visible on the western portion of the plateau appear again.

The prominent zone of ~NNW-SSE trending parallel ridges that run across the plateau can be traced southwards along the western side of the island of Nord-Fugløya, where it merges into a system of broad, E-W to NE-SW trending undulating ridges and trenches (Fig. 22a & b). This zone of parallel ridges thus reflect a major change in the orientation of morphologic elements on the strandflat, from dominantly NNW-SSE trending lineated morphology SW of Nord-Fugløya, to a dominantly NE-SE trending lineated morpholgy NE of Nord-Fugløya. This change is clearly visible on the aspect map (Fig. 22c).

Interpretation

The N-S to NNW-SSE trending diffuse and locally curved ridges north of Vanna, including similar morphologies on the western part of the raised plateau, are interpreted as the continuation of the TTG-gneiss foliation and possibly, meta-supracrustal lithologies analogue to the Skipsfjord Nappe rocks exposed onshore Vanna (Fig. 23). The wide zone of NNW-SSE trending parallel ridges, that may be traced northwest of Nord-Fugløya and north onto the raised plateau, is suggested to reflect the boundary zone between the crystalline Precambrian basement of the WTBC and the gently NW-dipping Caledonian thrust nappes present onshore Nord-Fugløya (Fig. 23; Roberts, 1974). Northeast of Nord-Fugløya, the observed NE-SW trending parallel ridges are interpreted to reflect the outcrop of Caledonian nappe foliation on the seabed. North of Nord-Fugløya, these ridges bend to a northwest trend, which is interpreted to be an apparent effect of the oblique truncation between the in general gently NW-dipping Caledonian foliation and the seabed.

The contact between the Caledonian rocks and the WTBC rocks must be present in the sound somewhere in between the islands of Spenna and Nord-Fugløya, as the two islands are comprised of WTBC rocks and Caledonian rocks, respectively (Fig. 24). The contact must thus trend NW-SE, parallel to the general morpho-tectonic trends present on the seabed within this sound. A possible continuation of this contact zone is visible on the raised plateau northwest of Nord-Fugløya, defined by the zone of ~NNW-SSE trending parallel ridges within the major trough (Fig. 23). Here, however, the zone does not separate ~NNW-SSE trending linear morphology, typical for basement lithologies, in the southwest from NE-SW trending linear morphology, typical for the Caledonian units, in the northwest, but rather obliquely truncate presumed basement lithologies on both sides. The exact location and southeastward trace of the Caledonian-WTBC contact, and its regional implications are discussed in a later section.

The south-facing escarpment delimiting the plateau and displacing the strandflat vertically by c.200m to the south is interpreted as a Late Palaeozoic-Mesozoic brittle fault. Consequently, this fault may be linked to the Vestfjord-Vanna Fault Complex, and thus imply that the WTBC rocks can be traced further northeastward along the Barents Sea margin (Fig. 24). This is also inferred from the N-S trend of the ductile basement fabrics visible on the raised plateau. The major brittle fault apparently displaces the strandflat and may therefore post-date the strandflat, (i.e. the Quaternary), thus inferring neotectonic activity.

Discussion

Above we have described and interpreted morpho-tectonic features visible on the strandflat offshore western Troms and compared them with local onshore ductile and brittle fabric elements. In order to further link and correlate these features, we have combined the two data-packages into a simplified onshore-offshore map of all the interpreted morpho-tectonic features along the studied portion of the WTBC and the transition to the Caledonian nappes in the northeast (Fig. 25). In the following, we will discuss the implications of these features in a regional context of onshore-offshore correlation and margin architecture.

A) Precambrian rocks and ductile fabrics

The morpho-tectonic elements observed on the strandflat clearly mimic onshore Precambrian basement structures in great detail, both in the form of interpreted lithologies and ductile structures. Dominant lithological elements such as the strongly foliated TTG-gneisses, more competent and massive granitic intrusions and meta-supracrustal belts can be tentatively identified and separated. Major ductile structures observed onshore, such as the prominent steep NW-SE trending, irregular and anastomosing Neoarchaean foliation in the TTG-gneisses and the complex Neoarchaean and later Svecofennian fold structures and ductile shear zones may be identified on the strandflat. In fact, even specific time-generations of folds and shear zones can be inferred in TTG gneisses on the strandflat bathymetry, including macro-scale isoclinal (D1), upright (D2) and steeply plunging folds (D3). Distinct zones of high-strain deformation that may represent terrane boundaries are identified on the strandflat (Fig. 25). These include the Astridal and Torsnes meta-supracrustal belts of the Senja Shear Belt, which are interpreted to continue NW onto the strandflat (Fig. 11b & c, Zwaan, 1995; Bergh et al., 2010). Further north, the possible offshore continuation of the Kvalsund shear zone is identified (Figs. 18 & 19). Onshore, the Kvalsund shear zone is related to a terrane boundary where adjacent gneisses are commonly heavily deformed and folded by upright, horizontal folds (Myhre et al., 2013). On the strandflat, along the trend of this zone, the occurrence of upright (D2) and steeply dipping (D3) macro folds (Fig. 25) indicate that the Kvalsund shear zone continues northwestward onto the strandflat. The great degree of similarity and correlation of morpho-tectonic elements on the strandflat with the onshore basement features (Fig. 25), suggests that the strandflat to a large extent is comprised of lithologies of WTBC affinity. In fact, the WTBC suite can be traced westward from the WTBC, all the way out to the western edge of the strandflat, from the the island of Senja in the south and northward to Nord-Fugløya. The contact zone to Caledonian rocks is interpreted to run just west and south of Nord-Fugløya (Figs. 24 & 25). The contact zone is clearly observed on the strandflat west and south of Nord-Fugløya (Fig. 23) and mirrored by a distinct change in the morpho-tectonic character of the seabed, strongly indicating that gently dipping Caledonian nappes and structures make up the strandflat northeast of this boundary.

B) Caledonian rocks and ductile fabrics

The Caledonian rocks of western Troms are outlined by flat-lying to gently NW-dipping thrust nappes with a marked structural difference relative to those of the WTBC rocks. In the northeastern part of the study area (Fig. 24), on the island of Nord-Fugløya and Arnøya, the onshore geology is overlain by Caledonian Kalak Nappe Complex units and northeast of these islands is the only area on the strandflat where Caledonian nappes are interpreted to crop out on the seafloor. Here, curved, parallel ridges that trend NE-SW dominate, as opposed to the NW-SE trending parallel ridges commonly observed within lithologies associated with the WTBC.

In a regional context, the onshore Caledonian-WTBC boundary of the SW Barents Sea margin (Figs. 1 & 2) is outlined by a zigzag pattern of NNE-SSW to ENE-WSW trending (mostly SE-dipping), brittle normal fault segments of the Vestfjord-Vanna Fault Complex

(Forslund, 1988; Olesen et al., 1997) and locally Caledonian thrust faults (on Senja and the northern parts of Ringvassøya). South of Nord-Fugløya, the orientation changes to a NNW-SSE trend, suggesting that the contact is no longer defined by coast-parallel brittle normal faults, but rather a thrust fault or a transfer fault zone of post-Caledonian age. The latter is supported by recent studies of Indrevær et al. (2013), which advocate the presence of a major sinistral transfer zone (Fugløya) of Late Palaeozoic-Mesozoic age, as a reactivated portion of the Proterozoic-Palaeozoic Bothnian-Kvænangen Fault Complex, running in the sound between Vanna and Nord-Fugløya. The wide zone of localised, parallel ridges observed on the raised plateau northeast of Vanna (Fig. 22) is therefore interpreted as the continuation of this transfer zone. However, since morphologies similar to that of exposed WTBC bedrock lithologies do occur on the eastern and western parts of the raised plateau, it is suggested that this zone, on the plateau, does not mark the direct continuation of the Caledonian-WTBC boundary, but rather reflect a Palaeoproterozoic meta-supracrustal belt, or the continuation of a pre-existing major, basement-seated ductile shear zone within WTBC rocks (Fig. 24). This strengthens the idea that the Fugløya transfer zone formed along a pre-existing zone of weakness within Precambrian basement rocks: The conspicuous overlap (Fig. 25) of (i) the Fugløya transfer zone, (ii) the contact between WTBC and Caledonian thrust nappes, (iii) a possible Svecofennian high-strain ductile shear zone and (iv) the Proterozoic-Palaeozoic Bothnian-Kvænangen Fault Complex, suggest that this zone may have played a major role in controlling and accommodating crustal deformation through a very long time span. This zone may have initiated during the Neoarchean and/or Palaeoproterozic orogenies, e.g. the Svecofennian, and later been overridden by thrust nappes during the Caledonian orogeny. Later Palaeozoic-Cenozoic crustal rifting, which led to the opening of the North-Atlantic Ocean, then potentially reactivated this zone as a transfer zone, displacing the Caledonian thrust nappes sinistrally and allowing Late Palaeozoic-Mesozoic brittle faults to step and change fault polarity across the transfer zone (Indrevær et al., 2013).

C) Post-Caledonian brittle structures

Post-Caledonian brittle faults are present throughout the studied passive margin (Indrevær et al., 2013) and are largely controlled by two major fault complexes, the partly onshore Vestfjord-Vanna Fault Complex and the offshore Troms-Finnmark Fault Complex that bound the WTBC horst (Gabrielsen et al., 1990; Olesen et al., 1997; Indrevær et al., 2013). The margin is segmented along strike by at least two Late Palaeozoic-Mesozoic transfer faults, the Senja Shear Zone and the Fugløya transfer zone (Olesen et al., 1997; Indrevær et al., 2013)

The two major fault complexes are both comprised of alternating NNE-SSE and ENE-WSW trending subsidiary fault zones (Gabrielsen et al., 1990; Olesen et al., 1997; Indrevær et al., 2013). A wide spectrum of irregular and linear trenches and escarpments truncate the strandflat bathymetry and the presumed bedrock structures, thus segmenting the strandflat into blocks. These features, including major boundary escarpments such as the westernmost scarp that defines the western edge of the strandflat, produce a zig-zag pattern of alternating ~NNE-ENE and ~ENE-WSW trending segments (Fig. 25) similar to those observed onshore (e.g. the VVFC) and on the deep shelf (e.g. the TFFC). We thus infer that these trenches and escarpments are in total, the result of Late Palaeozoic-Mesozoic rifting and brittle faulting that formed the present passive continental margin. The distribution of these faults, as evident from the bathymetry data, suggests that they are a part of a continuous system of horst-internal fault segments that link up onshore fault complexes with offshore complexes across the horst (Fig. 25).

Displacement

Estimating the amount of displacement across the trenches on the strandflat interpreted as brittle faults is important in order to understand their regional significance. In general, the VVFC, including the Vannareid-Brurøysund fault zone on Vanna have estimated amounts of displacement of 1-3km (Olesen et al., 1997). The less prevalent, linked fault system along the outer islands of the WTBC have estimated amounts of displacement of 100's of meters or less (Indrevær et al., 2013).

From this study, it is evident that the outer faults (e.g. the Bremneset, Tussøya and Hillesøya fault zones (Fig. 8 & 10) produce only weak bathymetric morphology. In areas where they are possible to trace onto the strandflat, they are not comparable in width nor depth with the many trenches that are observed on the strandflat. This suggests that the amount of displacement along the inferred fault-related trenches on the strandflat must have been greater than 100's of meters in order to produce wider damage zones (so that they may have been more heavily excavated by strandflat-forming processes and glacial erosion). However, the Vannareid-Brurøysund fault zone, for example, defines a topographic valley along its strike that is comparable in size with the offshore trenches (Fig. 21). The larger offshore trenches are thus suggested to have similar amounts of displacement as the VVFC and the Vannareid-Brurøysund fault zone (i.e. 1-3km). This is supported by the apparent dextral offset of the interpreted fold hinge zone running along the Kvalsund shear zone (Fig. 19b), which yielded an estimated amount of normal displacement of ~1.8km, down to the northwest.

The estimated displacement for interpreted brittle faults on the strandflat are thus similar to those estimated for the VVFC and implies that fault zones with displacements comparable with the VVFC may be widely distributed across the WTBC horst. Since very few fault zones comparable in displacement with the VVFC have been mapped onshore (e.g. Opheim & Andresen, 1989; Gagama, 2005), these major fault zones may tentatively be located within the larger sounds and fjords along the margin.

Timing of brittle faulting

Onshore, the brittle fault activity occurred in the Permian/Late-Triassic and came to a halt during early and deep stages of rifting as the rift activity propagated westward to offshore fault complexes in the Late Jurassic/Early Cretaceous (Davids et al., 2013; Indrevær et al., 2013; 2014). A similar westward progressive migration of fault activity may thus be expected for the brittle faults located on the strandflat. However, in order to preserve the entire WTBC horst as a uniform basement outlier, it is likely that most of these faults also became largely inactive after the Late Permian/Early Triassic rift event.

Several other indicators, which may shed light on the relative timing of fault segments and possible later reactivation, have been observed on the strandflat bathymetry. First, the relative timing of the alternating NNE-SSW and ENE-WSW trending brittle faults that constitute the two major fault complexes of the WTBC horst (Indrevær et al., 2013) can be inferred since both the NNE-SSW and ENE-WSW trending faults merge into parallelism with each other (Fig. 19a), suggesting that the two fault sets formed contemporaneously.

Secondly, the apparent sub-planar strandflat shows a vertical offset of c. 200m across inferred fault scarps. Examples include (i) the westernmost escarpment running along larger portions of the studied strandflat, which apparently has down-faulted the strandflat ~200m to the west (Fig. 20), (ii) the brittle fault zone that defines the southern limit of the raised plateau in Area 3, where the strandflat is displaced by ~200m down to the south (Fig. 22) and (iii) the presence of strandflat-internal smaller basins within Area 1 (Fig. 11b). The apparent ~200m vertical displacement across these scarps may be interpreted as the reactivation of the Late Palaeozoic-Mesozoic brittle faults after the formation of the strandflat, i.e. advocating Quarternary fault activity. Fenton (1991, 1994) and Muir Wood (1993) have listed criterias that may be used to separate neotectonic faults from older faults. The two most relevant criterions for this study is (i) that the amount of displacement is more or less constant along the entire length of the fault scarp and (ii) that the hight-to-length ratio of neotectonic fault scarps are typically in the range of 1:10.000 to 1:1.000, rarely exceeding the latter. The observed scarps do not show an increase in hight from the scarp tips to their centers (e.g. Fig. 20), thereby supporting their origin as neotectonic. However, if considering individual scarp segments, the hight-to-length ratio of the scarps does exceed 1:1000, typically falling in the range of c. 1:100 (Fig. 20). Only by considering the entire c. 200 km western boundary of the strandflat as one continuous fault scarp (Fig. 25) does the ratio approach 1:1.000.

The scarps may also be the result of glacitectonic ice-plucking of the hangingwall of the Late Palaeozoic-Mesozoic faults. Alternatively, the scarps may separate basement lithologies with contrasting susceptibility to the pre-Cretacous tropical weathering, thus leaving the apparent displacement of the strandflat across the scarps purely as a result of different amounts of Quarternary erosion.

D) Relation of bathymetry to present onshore topography and landscape forms

The analysis of aspect values (dip directions) for topographic surfaces dipping more than 5° (Fig. 5) shows that NNW-SSE, N-S and ENE-WSW trending slopes dominate on the strandflat. The N-S and ENE-WSW striking slopes make up the same zigzag pattern as evidently characterize the onshore WTBC-boundary fault zones and fault segments (i.e. VVFC) as well as the offshore Troms-Finnmark Fault Complex (Fig. 25; Indrevær et al., 2013). Onshore, the topography is dominated by NW-SE and NE-SW to E-W striking slopes, mirroring the orientations of ductile and brittle fabrics, respectively (Fig. 25, upper left corner). The SW Barents Sea margin landscape is therefore clearly influenced by Late Palaeozoic-Mesozoic brittle faulting, and to some extent, also Precambrian fabric elements. Both the topography and bathymetry show strong NW-SE trends close to the Senja Shear Belt and Fugløya transfer zone (Fig. 5 & 25), indicating the regional significance of these structures as terrane boundaries and later transfer zones (Olesen et al., 1997; Indrevær et al., 2013).

A similar study of the margin in Lofoten-Vesterålen has shown that the local topography is strongly influenced by brittle faults and fracture sets (Bergh et al., 2007b; Eig, 2008; Hansen, 2009). The brittle faults in Troms have similar orientation as faults and fractures in Lofoten-Vesterålen, but their effect on topography is apparently less. A possible explanation for this is the heterogeneous nature of the WTBC. In Lofoten, the basement is in large dominated by homogenous Palaeoproterozoic magmatic rocks (Griffin et al., 1978; Corfu, 2004). As few pre-existing zones of weakness existed for faults to utilize, the fault zones formed freely, in that they reflected the regional stress field and produced the alternating NNE-SSW and ENE-WSW trending fault zones as is present today. These were then the only zones of weakness that the main landscape forming element, the glaciers, could utilize and excavate during the Quaternary, enhancing the tectonic effect on topography. In the relatively heterogeneous WTBC, however, zones of weakness with more variable orientation, as produced by lithological boundaries, macro-scale folds, foliation and ductile shear zones were present and free to be utilized by faults and glaciers alike. As a result, the topography of the WTBC shows a larger degree of correlation with ductile basement structures and a lesser correlation with Late Palaeozoic-Mesozoic brittle faults than that of the Lofoten-Vesterålen margin.

Conclusions

- Morpho-tectonic features observed on the high-resolution bathymetry data covering the strandflat outboard Troms, mimics in great detail basement structures observed onshore, such as duplexes, steeply plunging tight folds, intrafolial macro-folds and shear zones, including the offshore continuations of high-strain meta-supracrustal belts. This strongly suggests that the lithologies of the WTBC are also present on the strandflat.
- The contact between WTBC lithologies with mainly sub-vertical N-S striking foliation and gently NW-dipping Caledonian thrust nappes is interpreted to run in the sound southwest of Nord-Fugløya, clearly visible as a distinct change in seabed morphology across the contact zone. The same sound marks the location of the Mesozoic Fugløya transfer zone, a possible reactivated portion of the Svecofennian Bothnian-Kvænangen Fault Complex, which has displaced the Basement-Caledonian contact sinistrally. The spatial overlap of these features suggests that the sound has exerted an important role in controlling and accommodating deformation of the margin through a very long time span.
- NNE-SSW to ENE-WSW trending trenches commonly truncate interpreted ductile structures on the strandflat and are interpreted as brittle faults based on their similar orientation as known onshore fault zones and fault zones on the continental shelf. Based on comparison of onshore fault zones impact on topography and the apparent offset of bedrock structures across a trench, the fault zones on the strandflat are suggested to have accommodated displacement on the order of kilometres.

- The structural relationship between faults of different orientation suggests that the Late Palaeozoic-Mesozoic fault zones, independent of their orientations, formed contemporaneous. Still, some interpreted fault zones on the strandflat defines escarpments that displaces the strandflat vertically with as much as 200m, inferring neo-tectonic activity. Alternatively, the vertical offset across the fault scarps may be due to glacitectonics, or lithological contrasts in susceptibility to pre-Cretaceous tropical weathering.
- Comparing topography and strandflat slope aspects reveals that the common orientations of basement structures and brittle faults onshore are reflected in the topography as well as the strandflat bathymetry. This supports a tectonic influence on the present day coastal landscape and the SW Barents Sea margin architecture.

Ackowledgements: This work was part of the Industrial PhD scheme organized by the Norwegian Research Council. The project is a collaboration between DONG E&P Norway and the University of Tromsø, financed by DONG E&P Norway and the Norwegian Research Council. We would like to express our gratitude to all persons involved from these institutions. We would also like to thank the Norwegian Mapping Authority and the Norwegian Armed Forces for sharing and allowing us to publish illustrations of the high-resolution bathymetry data.

References

Andresen, A. 1980: The age of the Precambrian basement in western Troms, Norway. *GFF*, *101*(4), 291-298.

Antonsdòttir, V. 2006: *Structural and kinematic analysis of the post-Caledonian Rekvika Fault Zone, Kvaløya, Troms*. Unpublished Master thesis, University of Tromsø, 84 pp.

Armitage, 2007: *Geological reconnaissance on Sandøya, West Troms Basement Complex, 04-07 September 2007*. Unpublished report, NunaMinerals A/S.

Armitage, P.E.B. & Bergh, S.G. 2005: Structural development of the Mjelde-Skorelvvatn Zone on Kvaløya, Troms: a metasupracrustal Shear Belt in the Precambrian West Troms Basement Complex, North Norway. *Norwegian Journal of Geology 85*, 117-132.

Bergh, S. G., Kullerud, K., Corfu, F., Armitage, P. E., Davidsen, B., Johansen, H. W., Pettersen, T & Knudsen, S. 2007a: Low-grade sedimentary rocks on Vanna, North Norway: a new occurrence of a Palaeoproterozoic (2.4-2.2 Ga) cover succession in northern Fennoscandia. *Norwegian Journal of Geology 87* (3), 301.

Bergh, S. G., Eig, K, Kløvjan, O. S., Henningsen, T., Olesen, O. & Hansen, J-A., 2007b: The Lofoten-Vesteralen continental margin: a multiphase Mesozoic-Palaeogene rifted shelf as shown by offshore-onshore brittle fault-fracture analysis. *Norwegian Journal of Geology 87*, 29 - 58.

Bergh, S. G., Kullerud, K., Armitage, P. E. B., Zwaan, K. B., Corfu, F., Ravna, E. J. K. & Myhre, P. I., 2010: Neoarchaean through Svecofennian tectono-magmatic evolution of the West Troms Basement Complex, North Norway. *Norwegian Journal of Geology*, *v. 90*, 21-48.

Bergh, S. G., Kullerud, K., Myhre, P. I., Corfu, F., Armitage, P. E. B., Zwaan, K. B., & Ravna, E. J. K. 2014: Archaean Elements of the Basement Outliers West of the Scandinavian Caledonides in Northern Norway: Architecture, Evolution and Possible Correlation with Fennoscandia. In *Evolution of Archean Crust and Early Life* (pp. 103-126). Springer Netherlands.

Binns, R.E., Chroston, P.N. & Matthews, D.W., 1980: Low-grade sediments on Precambrian gneiss on Vanna, Troms, Northern Norway. *Norges geologiske undersøkelse Bulletin 359*, 61-70.

Corfu, F. (2004). U–Pb age, setting and tectonic significance of the anorthosite–mangerite–charnockite–granite suite, Lofoten–Vesterålen, Norway. *Journal of Petrology, 45*(9), 1799-1819.

Corfu, F., Armitage, P. E. B., Kullerud, K. & Bergh, S. G., 2003: Preliminary U-Pb geochronology in the West Troms Basement Complex North Norway: Archaean and Palaeoproterozoic events and younger overprints. *Geological Survey of Norway, Bulletin 441*, 61-72.

Corner, G. D., 2005: Chapter 12. Atlantic coast and fjords. In: Seppälä, M. (ed.). The physical Geography of Fennoscandia, *Oxford Regional Environments Series*, Oxford University Press, 203-228.

Dahl, E., 1947: Litt om forholdene under og etter den siste istid i Norge. *Naturen*, *71*, 232-252.

Dahlgren, K. I., Vorren, T. O., Stoker, M. S., Nielsen, T., Nygård, A., & Petter Sejrup, H., 2005: Late Cenozoic prograding wedges on the NW European continental margin: their formation and relationship to tectonics and climate. *Marine and Petroleum Geology*, *22*(9), 1089-1110.

Davids, C., Wemmer, K., Zwingmann, H., Kohlmann, F., Jacobs, J. & Bergh, S.G. 2013: K–Ar illite and apatite fission track constraints on brittle faulting and the evolution of the northern Norwegian passive margin. *Tectonophysics 608*, 196–211.

Doré, A. G., Lundin, E. R., Fichler, C. & Olesen, O., 1997: Patterns of basement structure and reactivation along the NE Atlantic margin. *Journal of the Geological Society of London 154*, 85-92

Doré, A. G., Lundin, E. R., Jensen, L. N., Birkeland, Ø., Eliassen, P. E. & Fichler, C., 1999: Principal tectonic events in the evolution of the northwest European Atlantic margins. In: Fleet, A. J. & Boldy, S. A. R. (eds.), Petroleum Geology of Northwest Europe*: Proceedings of the 5th Conference*. *Geological Society of London*, 41-61.

Eig, K. 2008: *Onshore and offshore tectonic evolution of the Lofoten passive margin, North Norway*. Unpublished PhD thesis, University of Tromsø, 256 pp.

Fenton, C.H. 1991: Neotectonics and Palaeoseismicity in North West Scotland. Unpubl. Ph.D. Thesis, Univ. of Glasgow, 403 pp.

Fenton, C.H. 1994: Postglacial faulting in eastern Canada. Geological Survey of Canada Open file Report 2774, 98 pp.

Forslund, T. 1988: *Post-Kaledonske forkastninger i Vest-Troms, med vekt på Kvaløyslettaforkastningen, Kvaløya*. Unpublished Cand. Scient. thesis, University of Tromsø. 173 pp.

Gaal, G & Gorbatschev, R. 1987: An outline of the Precambrian evolution of the Baltic Shield. *Precambrian Research 35*, 15-52.

Gabrielsen, R. H. 1984: Long-lived fault zones and their influence on the tectonic development of the southwestern Barents Sea. *Journal of the Geological Society*, *141*(4), 651-662.

Gabrielsen, R.H., Færseth, R.B., Jensen, L.N., Kalheim, J.E. & Riis, F. 1990: Structural elements of the Norwegian continental shelf — Part I: the Barents Sea Region. *Norwegian Petroleum Directorate Bulletin 6*, 33 pp.

Gabrielsen, R. H., Braathen, A., Dehls, J. & Roberts, D. 2002: Tectonic lineaments of Norway. *Norwegian Journal of Geology, v. 82*, 153-174.

Gagama, M. F. V., 2005: *Strukturell analyse av post-kaledonske lineamenter ved Sifjorden, Vest-Senja, Troms*. Unpublished Master thesis, University of Tromsø, 85 pp.

Gjerlow, E. 2008: *Petrologi og alder av hoymetamorfe mafiske bergarter i det vestlige gneiskomplekset i Troms*. Unpublished Master thesis, University of Tromsø, 90 pp.

Grogan, P. & Zwaan, K.B. 1997: *Geologisk kart over Norge, berggrunnskart Helgøy, M 1:250 000,* Norges geologiske undersøkelse.

Griffin W. L., Taylor P. N., Hakkinen J. W., Heier K. S., Iden I. K., Krogh E. J. Malm O., Olsen K. I., Ormaasen D. E., and Tveten E., 1978: Archaean and Proterozoic crustal evolution in Lofoten-Vesterålen, N. Norway, *Journal of the Geological Society London, 135*, 629–647.

Hansen, J.-A. 2009: *Onshore-offshore tectonic relations on the Lofoten and Vesterålen Margin - Mesozoic to early Cenozoic structural evolution and morpological implications*. PhD thesis, University of Tromsø, 229 pp.

Hölttä, P. H., Balagansky, V., Garde, A. A., Mertanen, S., Peltonen, P., Slabunov, A.,Sorjonen-War, P. & Whitehouse, M. 2008: Archean of Greenland and Fennoscandia. *Episodes 31(1),* 13-19.

Indrevær, K., Bergh, S.G., Koehl, J.-B., Hansen, J.-A., Schermer, E.R. & Ingebrigtsen, A. 2013: Post-Caledonian brittle fault zones on the hyper-extended SW Barents Sea Margin: New insights into onshore and offshore margin architecture. *Norwegian Journal of Geology, Vol 93*, pp. 167-188.

Indrevær, K., Stunitz, H., & Bergh, S. G., 2014: On brittle normal faults along the SW Barents Sea margin: fault processes and implications for basement permeability and margin evolution. *Journal of the Geological Society, London, v. 171, no. 6.*

Johansen, H. 1987: *Forholdet mellom det prekambriske underlaget og overliggende sedimentære bergarter sørøst på Vanna, Troms*. Unpublished Cand. Scient thesis, University of Tromsø, 129 pp.

Lahtinen, R., Garde, A. A. & Melezhik, V. A., 2008: Paleoproterozoic evolution of Fennoscandia and Greenland. *Episodes 31(1),* 20.

Larsen, E., & Holtedahl, H., 1985: The Norwegian strandflat: A reconsideration of its age and origin. *Norsk geologisk tidsskrift*, *65*(4), 247-254.

Motuza, G., Motuza, V., Beliatsky, B. & Savva, E. 2001: *The Ringvassøya greenstone belt (Tromso, North Norway): implications for a Mesoarchaean subduction zone*. EUROPROBE time-slice symposium "Archaean and Proterozoic Plate Tectonics: Geological and Geophysical Records", St. Petersburg, Russia, October 1-November 3, 2001, 43-44.

Muir Wood, R. 1993: A review of the seismotectonics of Sweden. Swedish Nuclear Fuel and Waste Management Co. (SKB) Technical Report 93-13, 225 pp.

Myhre, P. I., Corfu, F., & Bergh, S., 2011: Palaeoproterozoic (2.0–1.95 Ga) pre-orogenic supracrustal sequences in the West Troms Basement Complex, North Norway. *Precambrian Research*, *186*(1), 89-100.

Myhre, P.I., Corfu, F., Bergh S.G. & Kullerud, K. 2013: U–Pb geochronology along an Archaean geotransect in the West Troms Basement Complex, North Norway. *Norwegian Journal of Geology, Vol 93*, pp. 1–24. Trondheim 2013, ISSN 029-196X.

Nansen, F., 1922: *The strandflat and isostasy (No. 11).* I kommission hos J. Dybwad.

Nyheim, H., Bergh, S. G., Krogh, E. J. & Zwaan, K. B. 1994: Torsnesskjærsonen i det vestlige (nord-norske) gneisterreng, Kvaløya, Troms; evidenser for kompleks skorpeforkortning og orogenparallelloblik strike-slip. *Nordic Geological Winter Meeting, Lulea*, p. 149.

Olesen, O., Torsvik, T. H., Tveten, E., Zwaan, K. B., Løseth, H. & Henningsen, T. 1997: Basement structure of the continental margin in the Lofoten-Lopphavet area, northern Norway: constraints from potential field data, on-land structural mapping and palaeomagnetic data, *Norwegian Journal of Geology, v. 77*, 15-30.

Opheim, J.A. and Andresen, A. 1989: Basement-cover relationships on northern Vanna, Troms, Norway. *Norwegian Journal of Geology*, *v. 69*(2), 67-81.

Ottesen, D., Dowdeswell, J. A., & Rise, L., 2005: Submarine landforms and the reconstruction of fast-flowing ice streams within a large Quaternary ice sheet: The 2500-km-long Norwegian-Svalbard margin (57–80 N). *Geological Society of America Bulletin*, *117*(7-8), 1033-1050.

Pedersen, B., R., S., 1997: *Strukturell analyse av en prekambrisk, duktilt deformert metasuprakrustalsone (Astridal-skjarsonen?) på NO-Senja, Troms*. Unpublished Cand. scient. thesis, University of Tromso, 166 pp.

Ramsay, D. M., Sturt, B. A., Jansen, Ø., Andersen, T. B., & Sinha-Roy, S. 1985: The tectonostratigraphy of western Porsangerhalvøya, Finnmark, north Norway. In: Gee, D.G. and Sturt, B.A. (eds): *The Caledonide Orogen: Scandinavia and related areas*. John Wiley, Chichester, UK, 611-619.

Reusch, H. (1894). Strandfladen, et nyt træk i Norges geografi. *Norges geologiske undersøkelse 14*, 1-12.

Rise, L., Bøe, R., Riis, F., Bellec, V. K., Laberg, J. S., Eidvin, T., Elvenes, S. & Thorsnes, T. 2013: The Lofoten-Vesterålen continental margin, North Norway: Canyons and mass-movement activity. *Marine and Petroleum Geology*, *45*, 134-149.

Roberts, D. 1974: Kartblad Hammerfest. Beskrivelse til det 1:250 000 berggrunnsgeologiske kart. *Norges geologiske undersøkelse Bulletin 301,* 66 p.

Roberts, D., 2003: The Scandinavian Caledonides: event chronology, palaeogeographic settings and likely modern analogues. *Tectonophysics 365*, p. 283-299

Roberts, D., Gee, D.G., 1985: An introduction to the structure of the Scandinavian Caledonides. In: Gee, D.G., Sturt, B.A. (Eds.), *The Caledonide Orogen—Scandinavia and Related Areas*. Wiley, Chichester, pp. 55– 68.

Roberts, D., Chand, S., & Rise, L. 2011: A half-graben of inferred Late Palaeozoic age in outer Varangerfjorden, Finnmark: evidence from seismic reflection profiles and multibeam bathymetry. *Norwegian Journal of Geology 91*(3), 193-202.

Rydningen, T.A., Vorren T.O., Laberg, J.S. & Kolstad, V. 2013: The marine-based NW Fennoscandian ice sheet: glacial and deglacial dynamics as reconstructed from submarine landforms. *Quaternary Science Reviews, v. 68*, 126-141.

Thorsnes, T, Erikstad, L., Dolan, M. F. J. & Bellec, V. K. 2009: Submarine landscapes along the Lofoten-Vesterålen-Senja margin, northern Norway. *Norwegian Journal of Geology*, *v. 89* (1-2), 5-16.

Thorstensen, L. 2011: *Land-sokkel korrelasjon av tektoniske elementer i ytre del av Senja og Kvaløya i Troms*. Unpublished Master thesis, University of Tromsø, 107 pp.

Vorren, T. O., Edvardsen, M., Hald, M., & Thomsen, E., 1983: Deglaciation of the continental shelf off southern Troms, North Norway. *Norges Geologiske Undersøkelse Bulletin*, (70), 173-187.

Zwaan, K. B., 1989: Berggrunnsgeologisk kartlegging av det prekambriske grønnsteinsbeltet pa Ringvassoy, Troms. *Norges geologiske undersøkelse Rapport 89*.101.

Zwaan, K. B. 1995: Geology of the West Troms Basement Complex, northern Norway, with emphasis on the Senja Shear Belt: a preliminary account. *Geological Survey of Norway, Bulletin 427*, 33-36.

Zwaan K. B., Fareth, E. & Grogan, P.W. 1998: *Geologisk kart over Norge, berggrunnskart TROMSØ, M 1:250.000*. Norges geologiske undersøkelse.

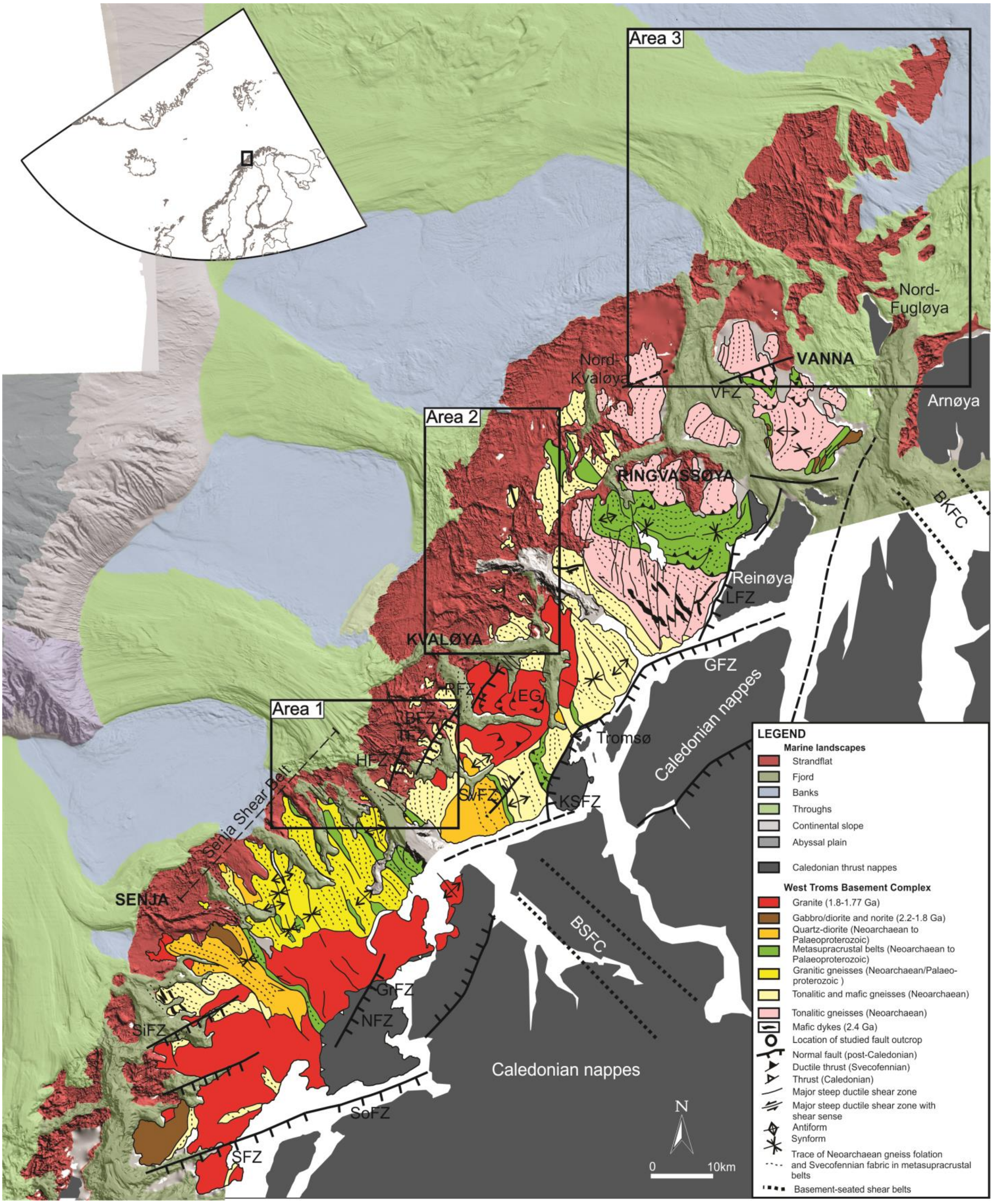

Area 1
Area 2
Area 3
Nord-Fugløya
VANNA
Nord-Kvaløya
VFZ
Arnøya
RINGVASSØYA
BKFC
Reinøya
LFZ
KVALØYA
GFZ
Caledonian nappes
BFZ
EG
Tromsø
HFZ
SvFZ
KSFZ
Senja Shear Belt
SENJA
BSFC
GiFZ
NFZ
SiFZ
SoFZ
SFZ
Caledonian nappes
N
0
10km
LEGEND
Marine landscapes
Strandflat
Fjord
Banks
Throughs
Continental slope
Abyssal plain
Caledonian thrust nappes
West Troms Basement Complex
Granite (1.8-1.77 Ga)
Gabbro/diorite and norite (2.2-1.8 Ga)
Quartz-diorite (Neoarchaean to Palaeoproterozoic)
Metasupracrustal belts (Neoarchaean to Palaeoproterozoic)
Granitic gneisses (Neoarchaean/Palaeo-proterozoic)
Tonalitic and mafic gneisses (Neoarchaean)
Tonalitic gneisses (Neoarchaean)
Mafic dykes (2.4 Ga)
Location of studied fault outcrop
Normal fault (post-Caledonian)
Ductile thrust (Svecofennian)
Thrust (Caledonian)
Major steep ductile shear zone
Major steep ductile shear zone with shear sense
Antiform
Synform
Trace of Neoarchaean gneiss folation and Svecofennian fabric in metasupracrustal belts
Basement-seated shear belts

Figure 1 (previous page): Detailed geological map of the West Troms Basement Complex showing main Archaean-Palaeoproterozoic fabrics and post-Caledonian brittle normal faults that separate the basement horst from down-dropped Caledonian nappes to the east (after Bergh et al., 2010). Offshore, marine landscape types are given, including the lateral distribution of the strandflat (mareano.no). Three areas of focus of the present paper are marked. Abbreviations: BFZ = Bremneset fault zone, BKFC=Bothnian-Kvænangen Fault Complex, BSFC=Bothnian-Senja Fault Complex, EG=Ersfjord Granite, GFZ=Grøtsundet fault zone, GrFZ=Grasmyrskogen fault zone, HFZ = Hillesøy fault zone, KSFC=Kvaløysletta-Straumsbukta fault zone, LFZ=Langsundet fault zone, NFZ=Nybygda fault zone, RFZ=Rekvika fault zone, SFZ=Stonglandseidet fault zone, SiFZ=Sifjorden fault zone, SoFZ=Solbergfjorden fault zone, SvFZ=Skorelvvatn fault zone, TFZ=Tussøya fault zone, VFZ=Vannareid-Brurøysund fault zone, VVFC=Vestfjorden-Vanna Fault Complex.

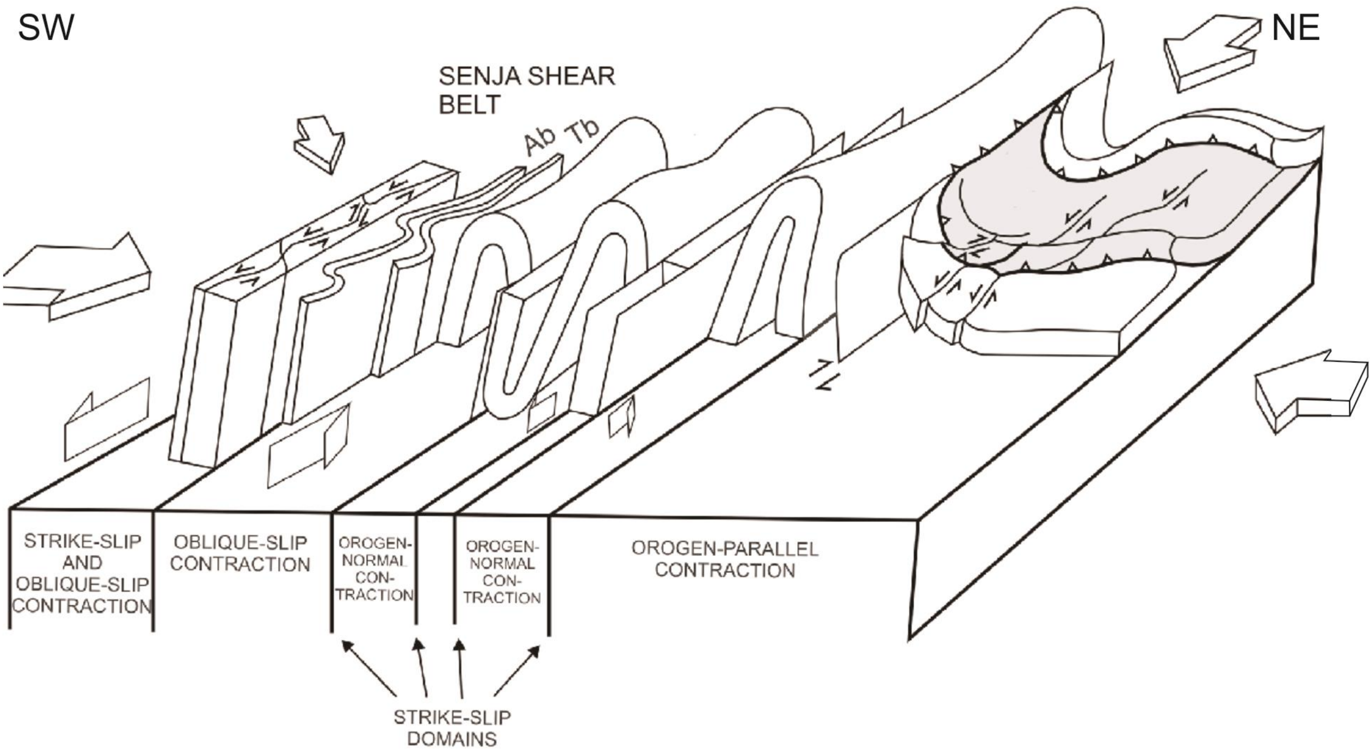

Figure 2: Schematic (not to scale) geometric/kinematic model for the development of Svecofennian structures observed in the WTBC. Early-stage formation of NE-directed thrusts and a low-angle main mylonitic foliation in the metasupracrustal belts was continued by orthogonal NE-SW contraction that produced upright macro-folds with steep limbs. Late-stage Svecofennian tectonism involved NE-SW orthogonal and/or oblique to orogen-parallel contraction (NW-SE) and mostly sinistral strike-slip reactivation of steep macro-fold limbs, e.g. in the Senja Shear Belt. The eastern, more flatlying macro-fold hinges accommodated NW-SE shortening and SE-directed thrusting. From Bergh et al. (2010). Abbreviations: Ab=Astridal belt, Tb=Torsnes belt.

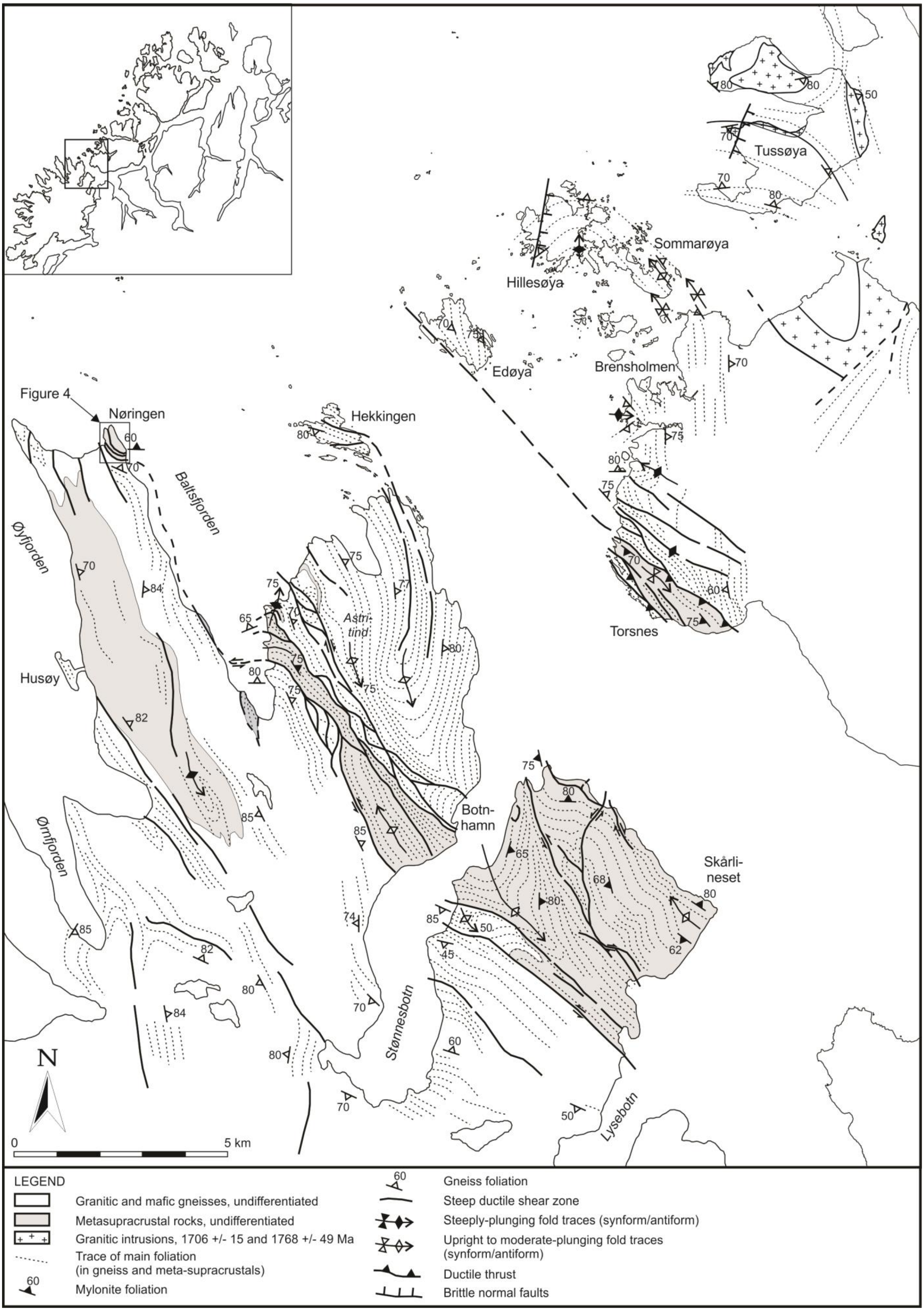

Tussøya
Sommarøya
Hillesøya
Edøya
Brensholmen
Figure 4
Nøringen
Hekkingen
Baltsfjorden
Øyfjorden
Astritind
Husøy
Torsnes
Botn-
hamn
Skårli-
neset
Ømfjorden
Stønnesbotn
Lysebotn
N
0
5 km
LEGEND
Granitic and mafic gneisses, undifferentiated
Metasupracrustal rocks, undifferentiated
Granitic intrusions, 1706 +/- 15 and 1768 +/- 49 Ma
Trace of main foliation
(in gneiss and meta-supracrustals)
Mylonite foliation
Gneiss foliation
Steep ductile shear zone
Steeply-plunging fold traces (synform/antiform)
Upright to moderate-plunging fold traces
(synform/antiform)
Ductile thrust
Brittle normal faults

Figure 3 (previous page): Tectonic map of the Senja Shear Belt in northeastern Senja and southwestern Kvaløya, illustrating the lens-shaped architecture of the Astridal and Torsnes belts. Note macro-scale folds in the adjacent tonalitic gneisses where fold hinges are rotated into parallelism with the trace of the Astridal belt. The map is modified from Nyheim et al. (1994), Pedersen (1997), Zwaan et al. (1998), Corfu et al. (2003) and Bergh et al. (2010).

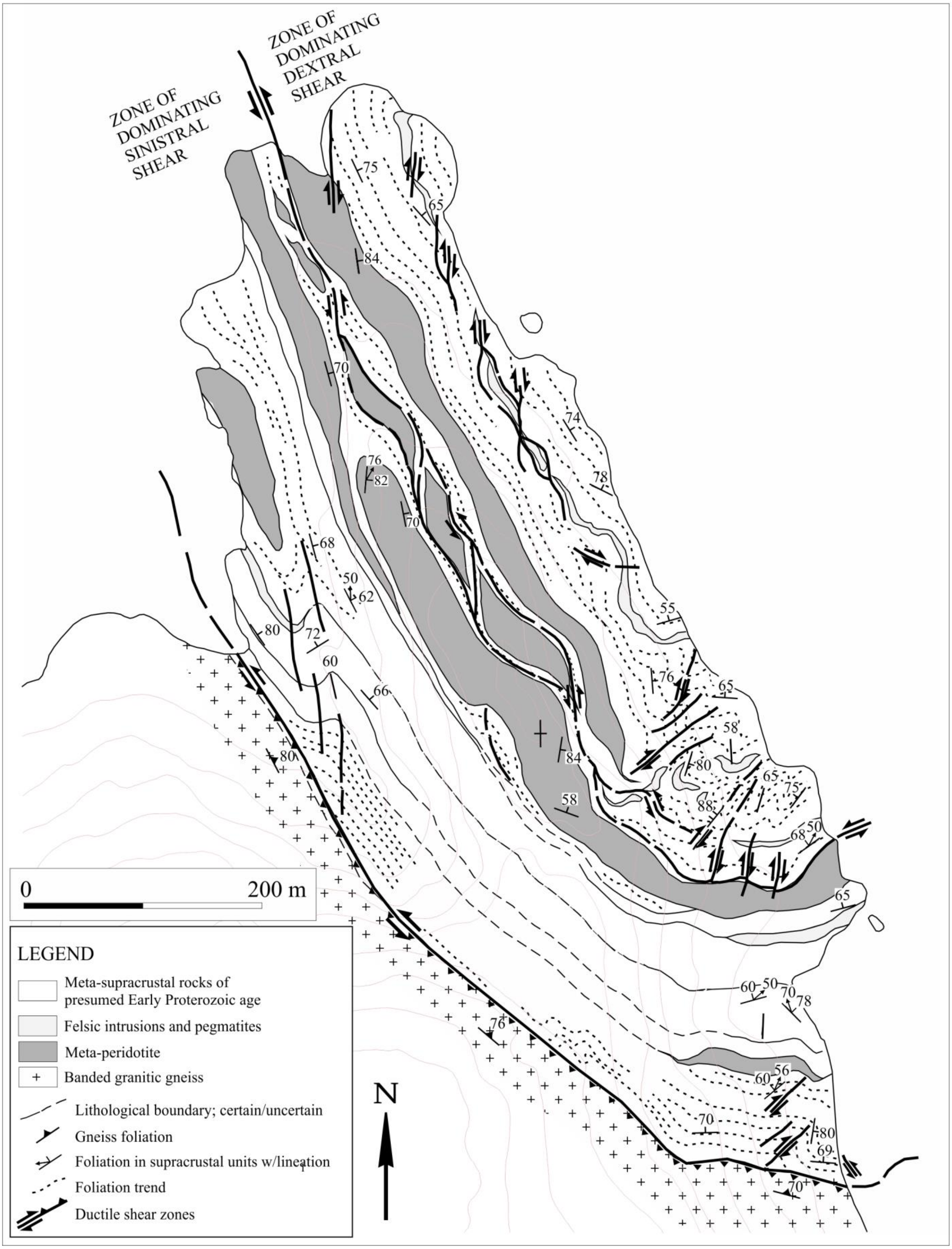

Figure 4: Detailed geological and structural map covering meta-supracrustal rocks that crop out at Nøringen. Note how meta-peridotites are sinistrally duplexed. Simplified from Pedersen (1997).

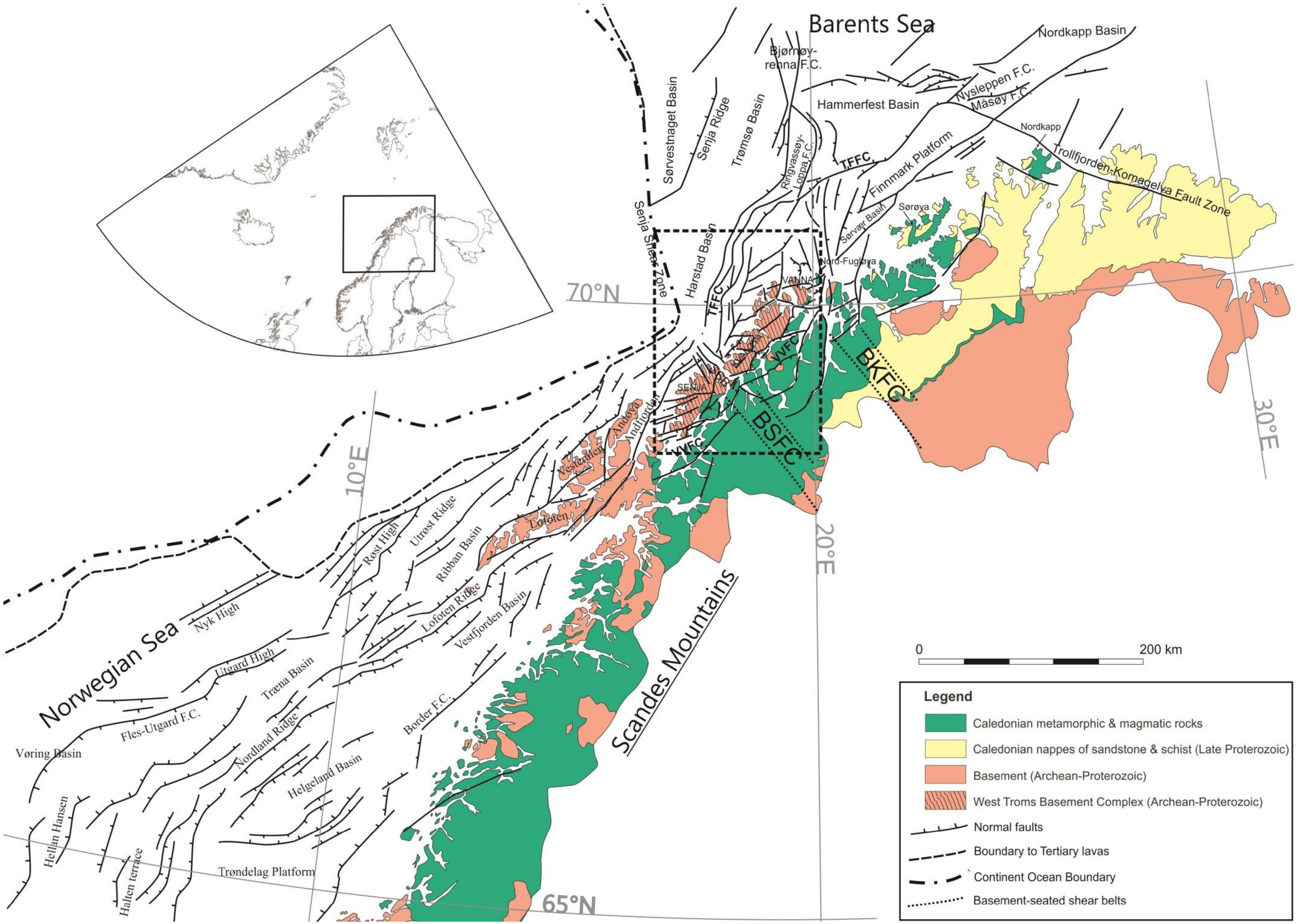

Figure 5: Regional onshore-offshore tectonic map and setting of the Lofoten-Vesterålen archipelago and the SW Barents Sea margin (after Blystad et al., 1995; Mosar et al., 2002; Bergh et al., 2007a; Faleide et al., 2008; Hansen et al., 2012; Indrevær et al., 2014). Onshore geology is from the Geological Survey of Norway. Areas of focus in are outlined. Abbreviations: BKFC=Bothnian-Kvænangen Fault Complex, BSFC=Bothnian-Senja Fault Complex, TFFC=Troms-Finnmark Fault Complex, VVFC=Vestfjorden-Vanna Fault Complex.

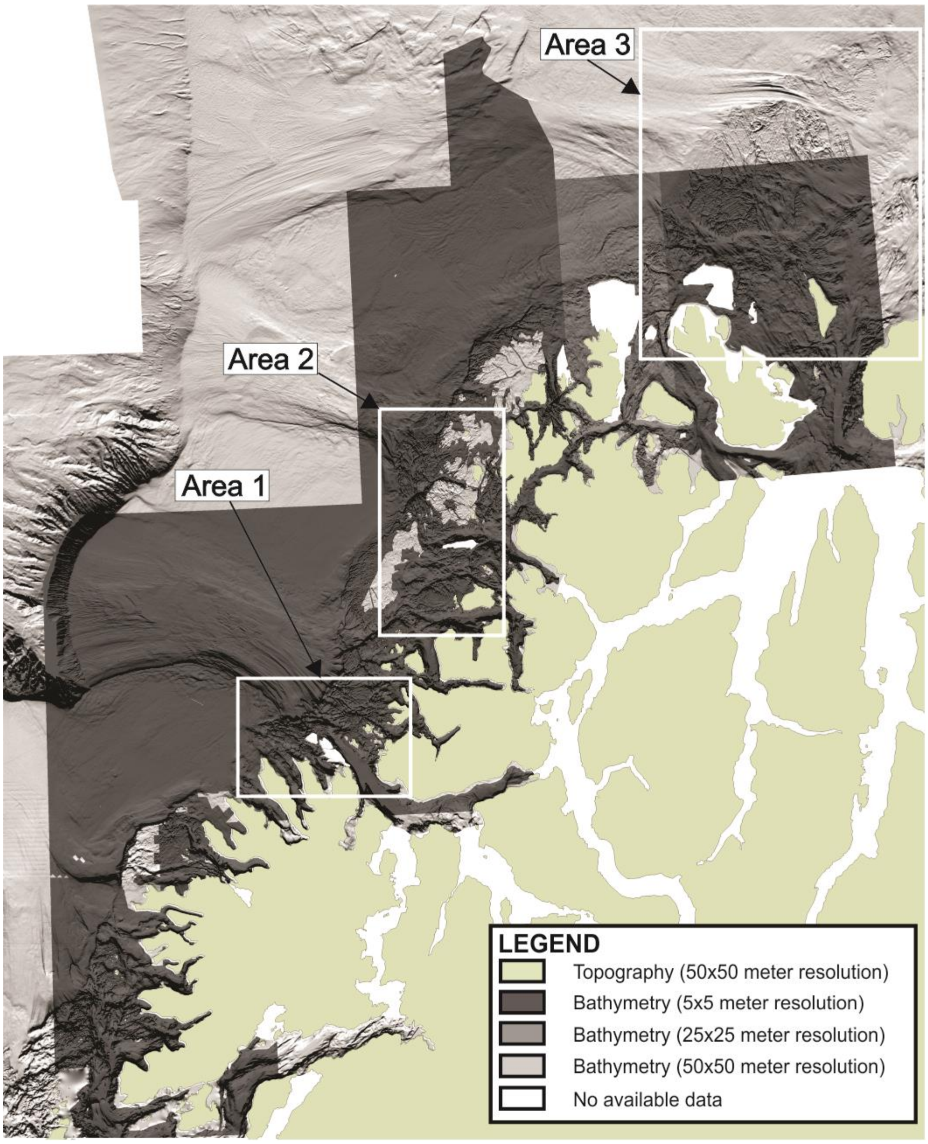

Figure 6: Overview of the available bathymetry data and its resolution. Note that there are several gaps in the 5x5m resolution data set covering the strandflat.

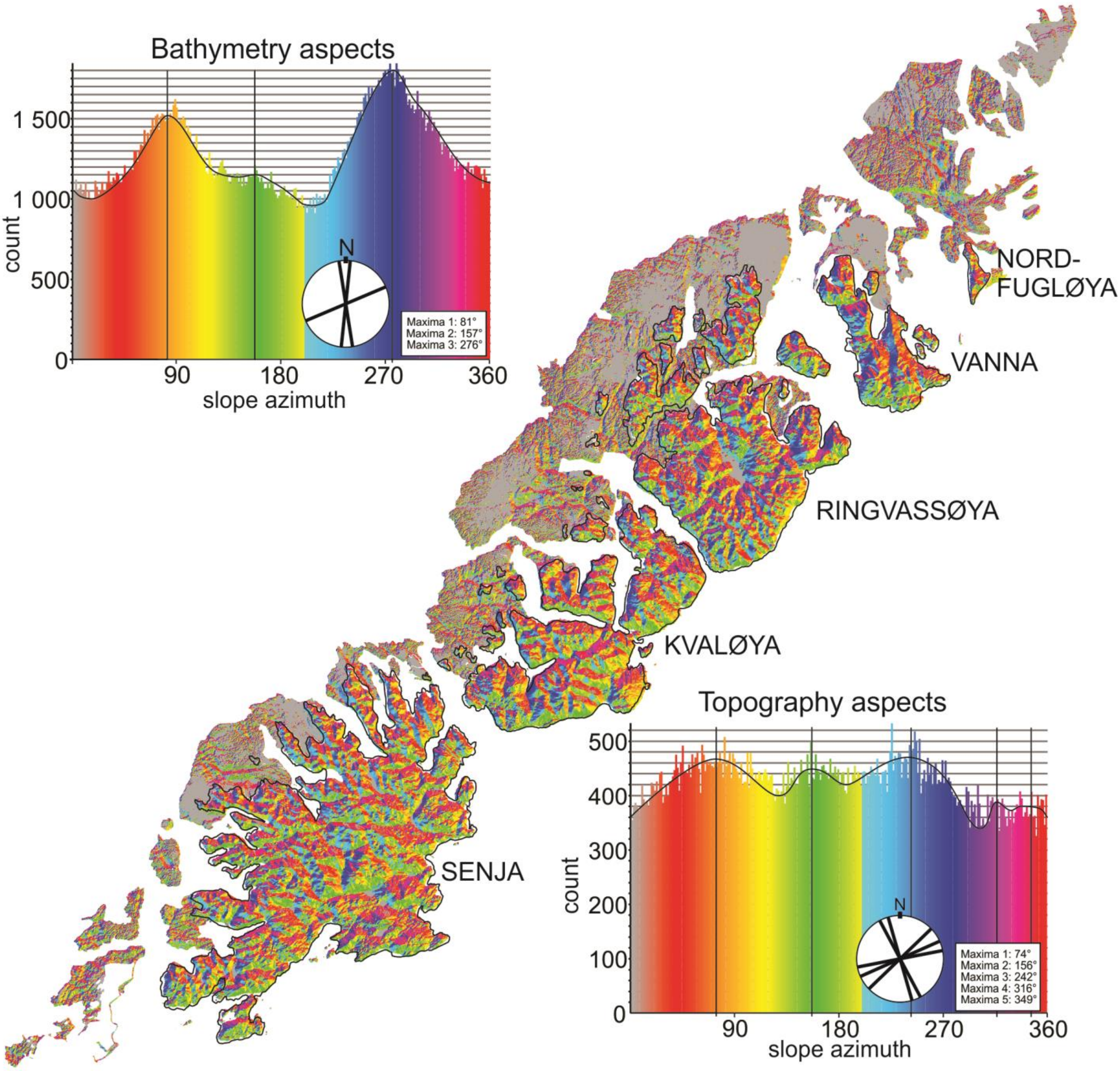

Figure 7: Aspect analysis of slopes steeper than 5°, for the outer islands and strandflat off Troms. Bathymetry (strandflat) aspects and topography aspects are shown separately (black lines indicate a running average of the aspects). Circular insets represent simplified rose diagrams. The analysis shows that N-S and NE-SW trending slopes are common on the strandflat, while NW-SE and NE-SW to E-W trending slopes are common onshore. These orientations are the same as orientations that dominate both ductile and brittle structures onshore.

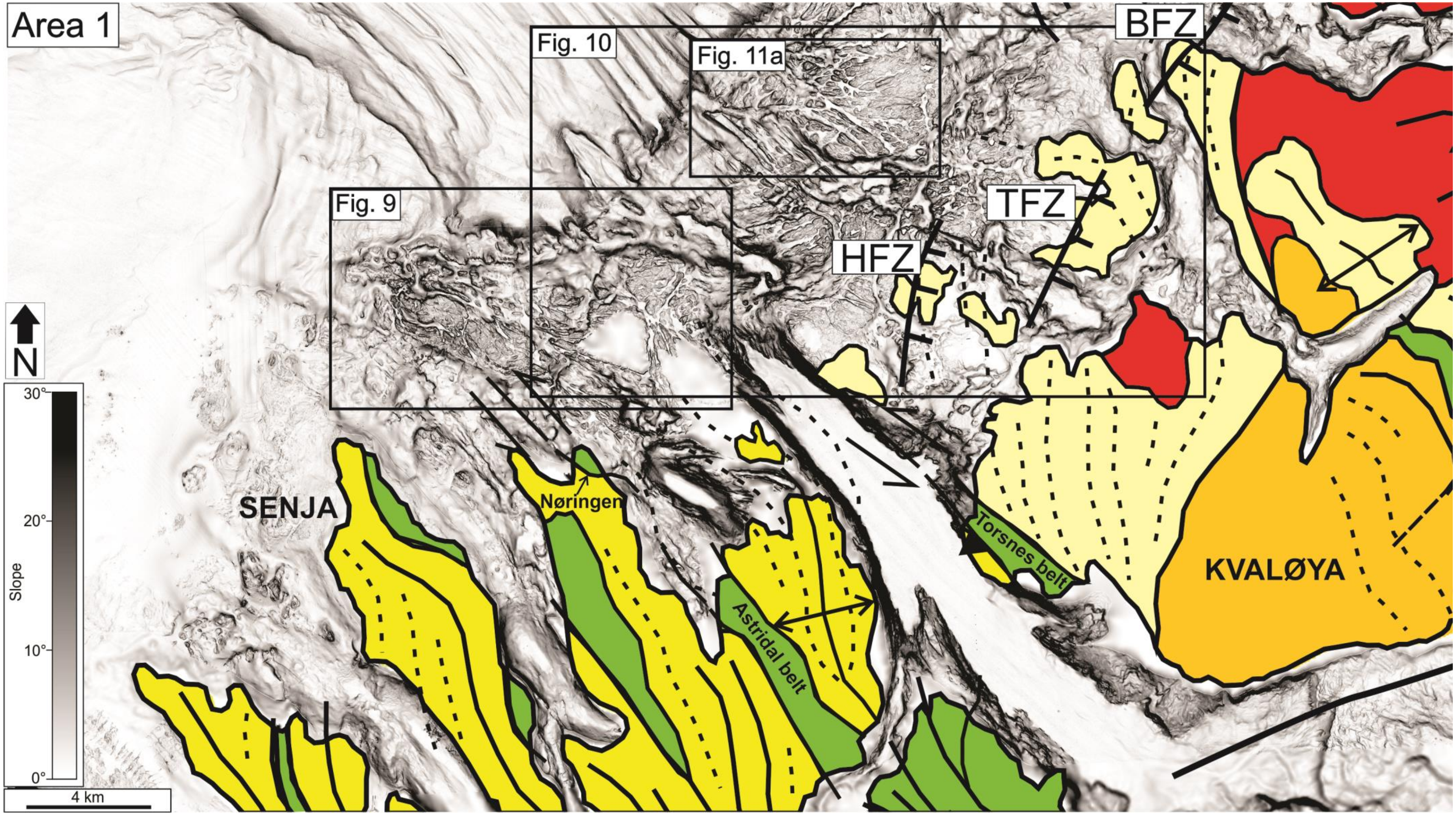

Figure 8: Overview of Area 1 covering the strandflat outboard northern portions of Senja and the southeastern portions of Kvaløya. Onshore geology from Bergh et al., (2010). Figures 9 and 10 are outlined.

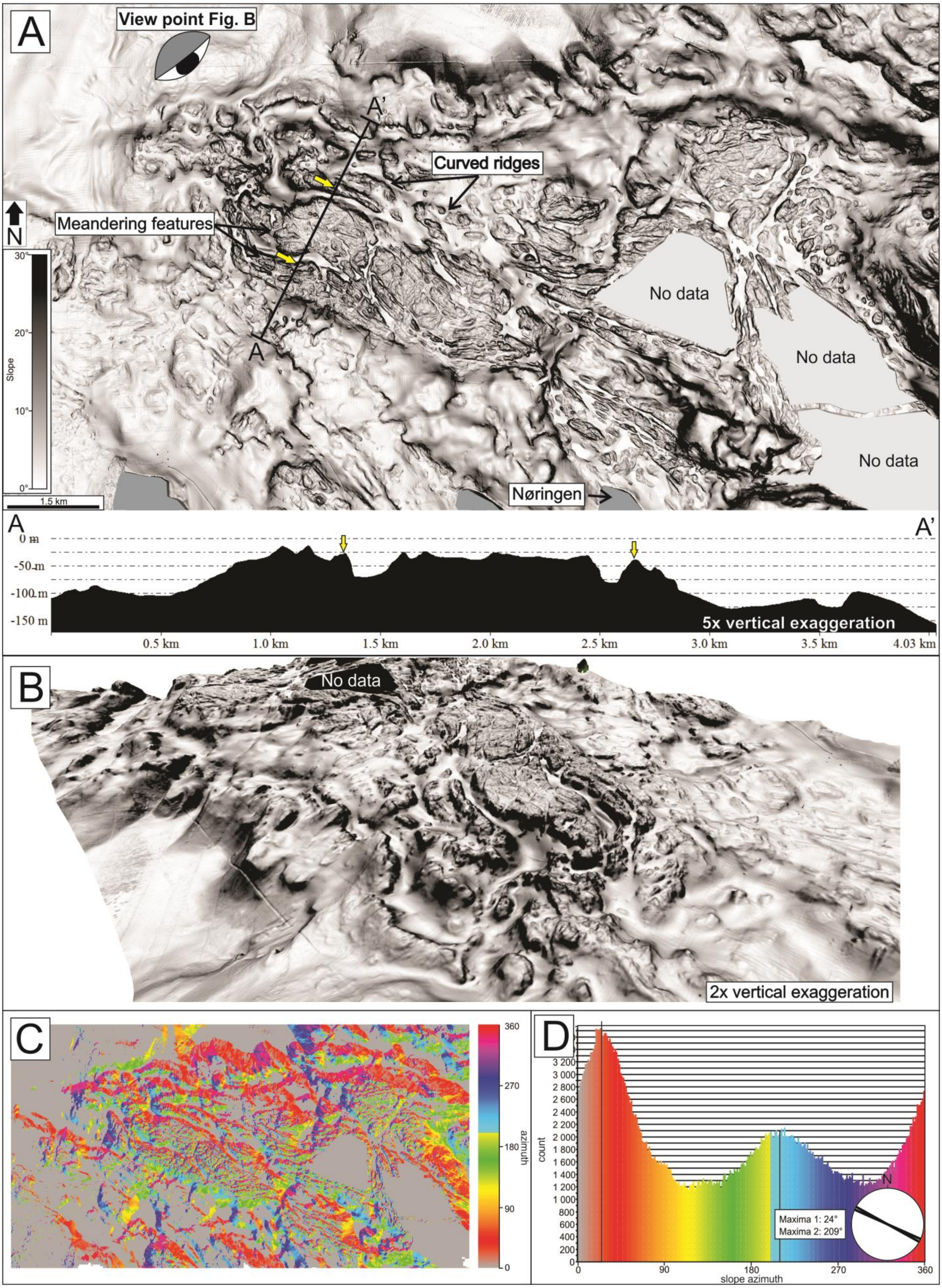
A
View point Fig. B
A'
Curved ridges
Meandering features
N
Slope
30°
20°
10°
0°
1.5 km
A
No data
No data
No data
Nøringen
A
A'
0 m
-50 m
-100 m
-150 m
5x vertical exaggeration
0.5 km
1.0 km
1.5 km
2.0 km
2.5 km
3.0 km
3.5 km
4.03 km
B
No data
2x vertical exaggeration
C
azimuth
360
270
180
90
0
D
count
slope azimuth
Maxima 1: 24°
Maxima 2: 209°
N

Figure 9 (previous page): Detailed illustrations of the strandflat within Area 1 (see Fig. 8 for location). (**a**) Dip map covering the strandflat with location of cross-section given and shown below. Yellow arrows indicate points of reference. Note the NW-SE trending meandering feature. Point of view for 3D illustration is marked. (**b**) 3D bathymetry illustration of the subarea, which highlights the meandering nature of the seabed morphology. (**c**) Aspect map and (**d**) histogram showing the prefered dip direction for slopes steeper than 5°. The preferred strikes of slopes from the aspect analysis are shown in the small circular insets (simplified rose diagrams).

Figure 10 (next page): Detailed illustrations of the strandflat within Area 1 (see Fig. 8 for location). (**a**) Dip map bathymetry data covering the strandflat with onshore portions of the subarea covered by aerial photographs. Locations of cross-sections are shown and given below. Yellow arrows indicate points of reference. Point of view for 3D illustration is marked. (**b**) 3D illustration of the subarea, which highlights the continuation of the Torsnes belt with a notable rounded z-shape. (**c**) Aspect map and (**d**) histogram showing the prefered direction of dips for slopes steeper than 5°. Grey line shows the preferred aspects of the topography (not to scale along the Y-axis). The preferred strikes of slopes from the aspect analysis are shown in the small circular insets (simplified rose diagrams, grey lines shows *topography* maxima).

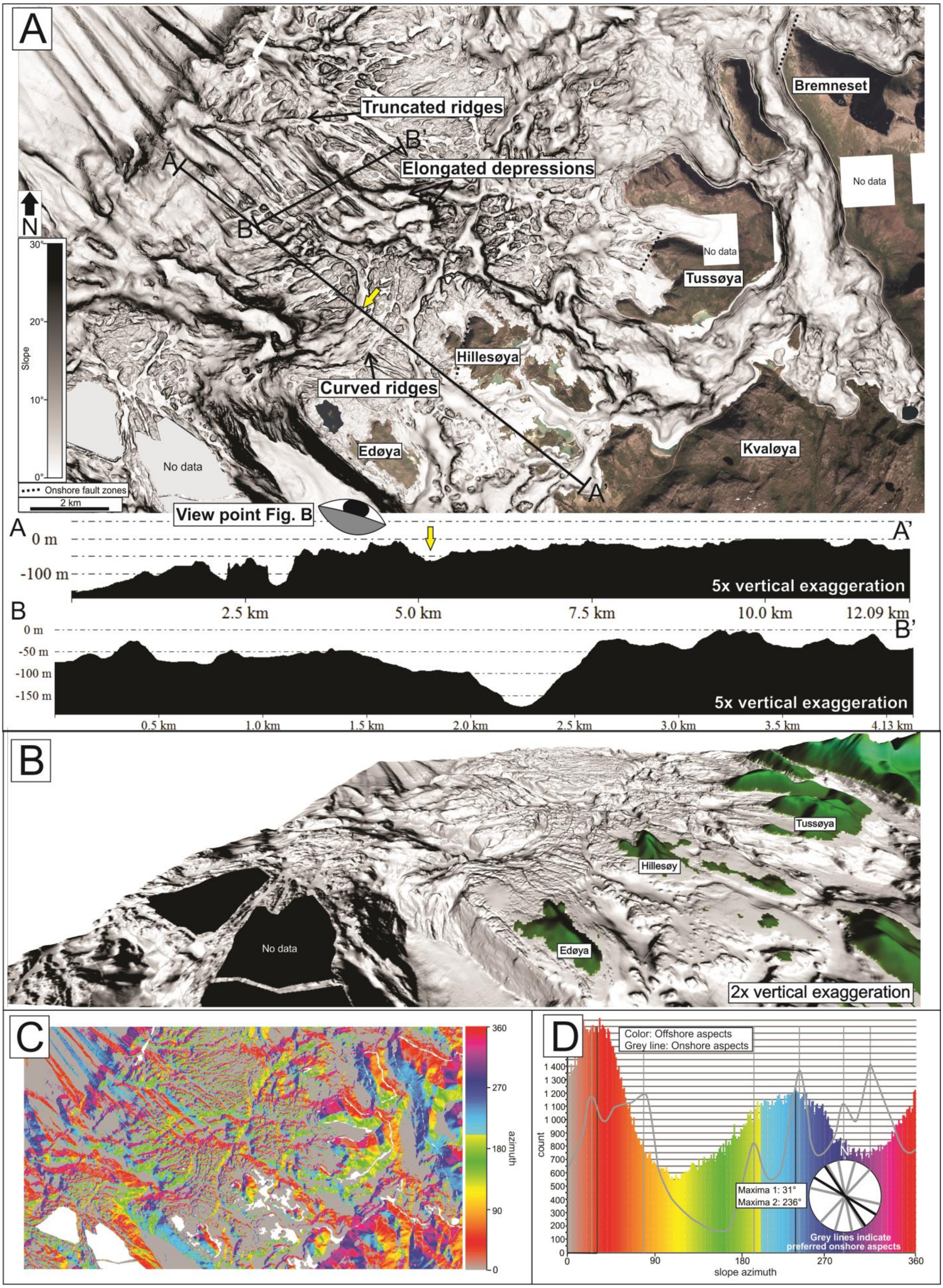

A
Truncated ridges
Elongated depressions
B'
B
A
A'
N
Slope
30°
20°
10°
0°
Onshore fault zones
2 km
Bremneset
No data
No data
Tussøya
Hillesøya
Curved ridges
Edøya
Kvaløya
No data
View point Fig. B
0 m
-100 m
5x vertical exaggeration
2.5 km
5.0 km
7.5 km
10.0 km
12.09 km
0 m
-50 m
-100 m
-150 m
0.5 km
1.0 km
1.5 km
2.0 km
2.5 km
3.0 km
3.5 km
4.13 km
B
Tussøya
Hillesøy
Edøya
No data
2x vertical exaggeration
C
azimuth
360
270
180
90
0
D
Color: Offshore aspects
Grey line: Onshore aspects
count
Maxima 1: 31°
Maxima 2: 236°
N
Grey lines indicate preferred onshore aspects
slope azimuth

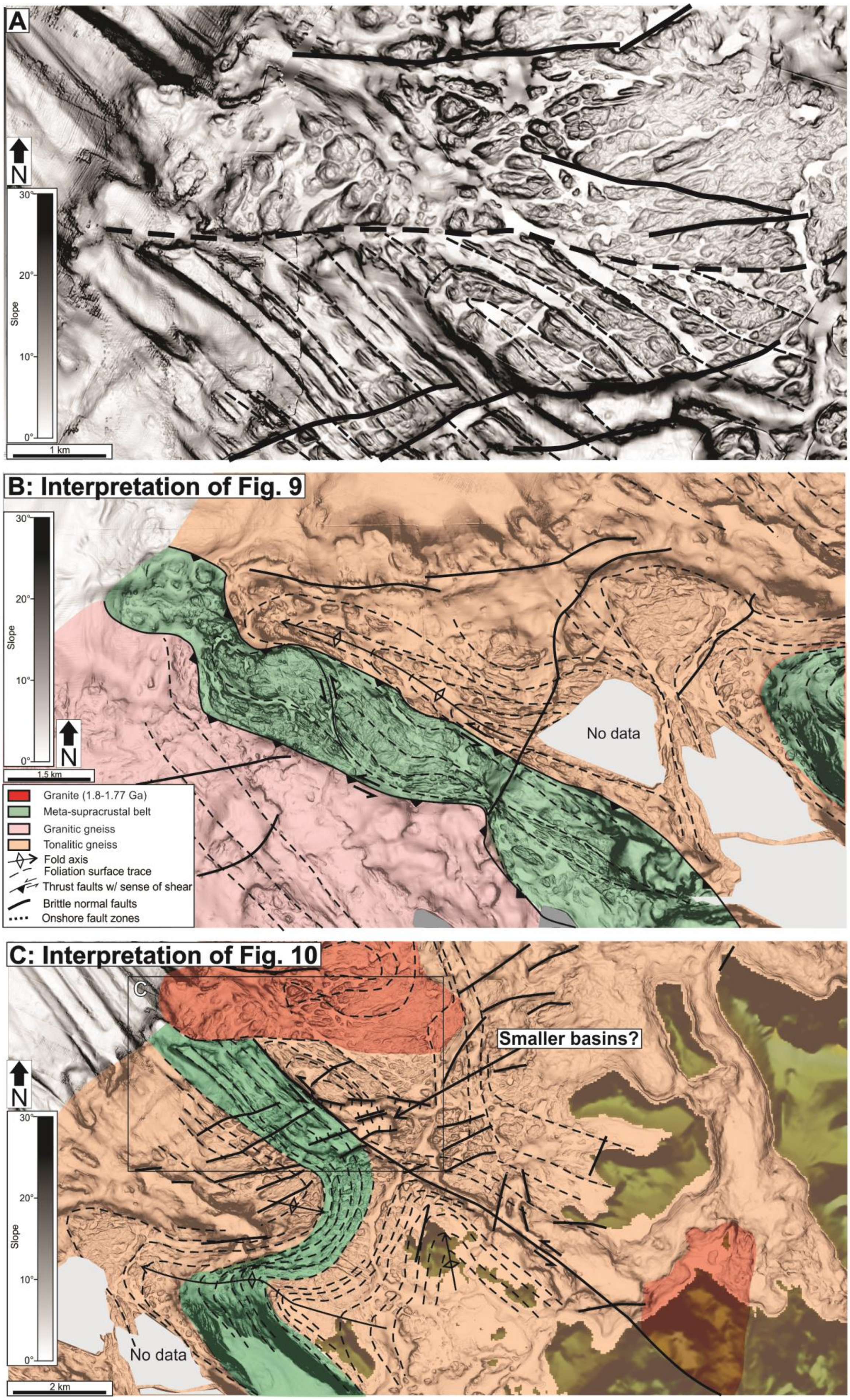
A
N
30°
20°
Slope
10°
0°
1 km
B: Interpretation of Fig. 9
30°
20°
Slope
10°
0°
N
1.5 km
No data
Granite (1.8-1.77 Ga)
Meta-supracrustal belt
Granitic gneiss
Tonalitic gneiss
Fold axis
Foliation surface trace
Thrust faults w/ sense of shear
Brittle normal faults
Onshore fault zones
C: Interpretation of Fig. 10
C
Smaller basins?
N
30°
20°
Slope
10°
0°
No data
2 km

Figure 11 (previous page): Interpretative mapping of lithologies and structures covering the strandflat in Area 1 (see Fig. 8 for locations), based on correlation with known onshore structures. (**a**) Detailed outline of the northern portion of the offshore continuation of the Torsnes belt, which is truncated by a E-W trending lineament, separating homogenous and unfoliated rocks interpreted as a granitic intrusion in the north from the well-foliated rocks in the south. (**b**) The meandering feature visible northwest of Nøringen is interpreted as the offshore continuation of the Nøringen and Astridal belt. The belt is sinistrally duplexed and bounded by drag-folded gneiss to the north, consistent with an overall sinstral sense of shear. (**c**) Interpretative mapping of the northern portion of Area 1. The offshore continuation of the Torsnes belt is folded into a rounded z-shape and runs in the north parallel to a sinistral shear zone that may be traced from land.

Figure 12 (next page): Overview of Area 2 covering the strandflat outboard northern portions of Kvaløya and west of Ringvassøya, including the islands of Vengsøya, Gjøssøya, Rebbenesøya, Sandøya and Sørfugløya. Onshore geology from Bergh et al. (2010). Figures 13 to 17 are outlined by boxes and the location of two cross-sections are given and shown below. Inset: Simplified geological map of Sandøya. Note the NNE-SSW trending quartzite layer that dominates the eastern portion of the island. From Armitage (2007).

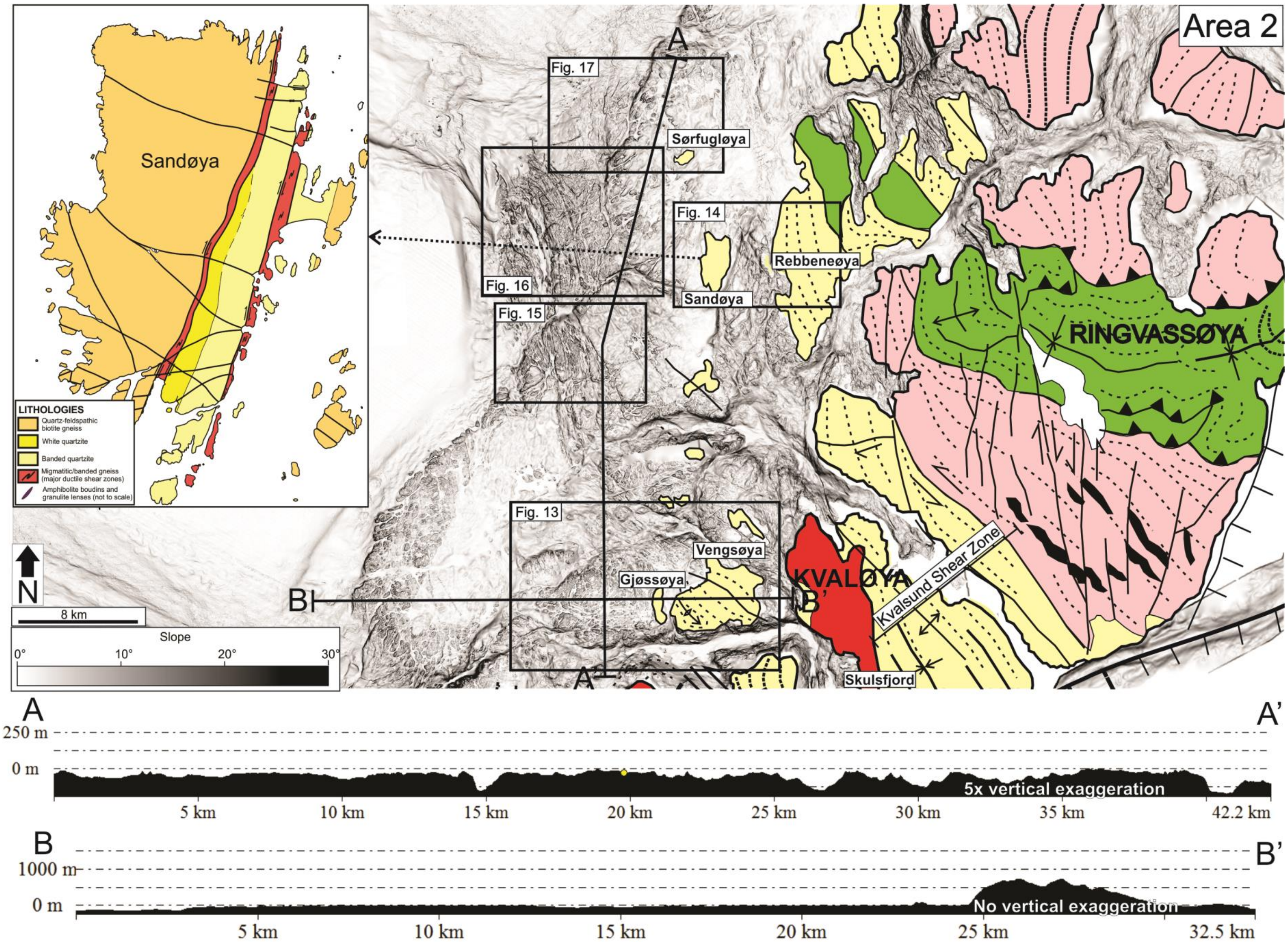
Area 2
Sandøya
LITHOLOGIES
Quartz-feldspathic biotite gneiss
White quartzite
Banded quartzite
Migmatitic/banded gneiss (major ductile shear zones)
Amphibolite boudins and granulite lenses (not to scale)
A
Fig. 17
Sørfugløya
Fig. 16
Fig. 14
Rebbeneøya
Sandøya
Fig. 15
RINGVASSØYA
Fig. 13
Vengsøya
Gjøssøya
KVALØYA
Kvalsund Shear Zone
Skulsfjord
B
B'
A'
N
8 km
Slope
0°
10°
20°
30°
A
A'
250 m
0 m
5x vertical exaggeration
5 km
10 km
15 km
20 km
25 km
30 km
35 km
42.2 km
B
B'
1000 m
0 m
No vertical exaggeration
5 km
10 km
15 km
20 km
25 km
32.5 km

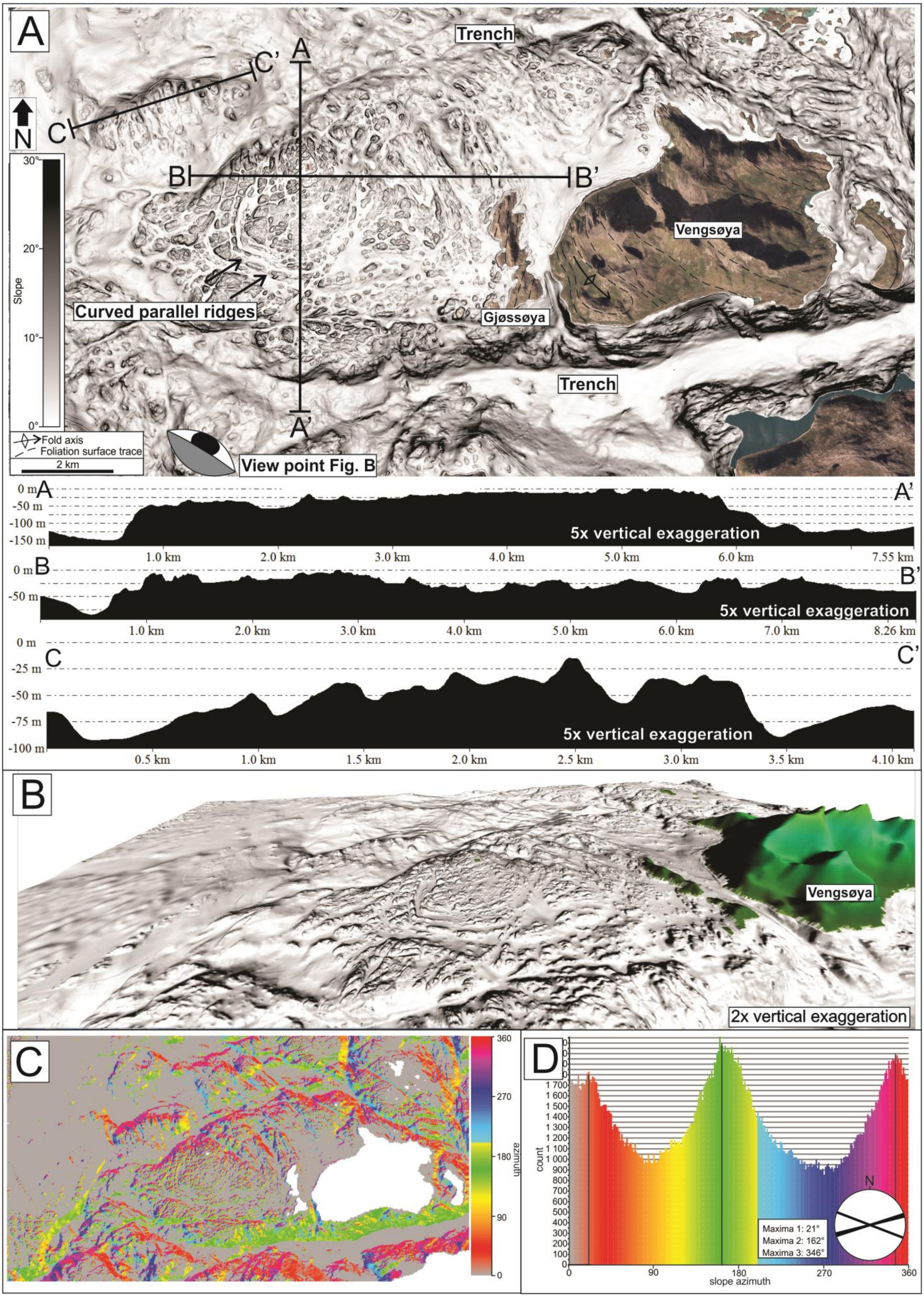
A
Trench
A
C'
C
N
B
B'
30°
20°
10°
0°
Slope
Vengsøya
Curved parallel ridges
Gjøssøya
Trench
A'
Fold axis
Foliation surface trace
2 km
View point Fig. B
0 m
-50 m
-100 m
-150 m
A
A'
5x vertical exaggeration
1.0 km
2.0 km
3.0 km
4.0 km
5.0 km
6.0 km
7.55 km
0 m
-50 m
B
B'
5x vertical exaggeration
1.0 km
2.0 km
3.0 km
4.0 km
5.0 km
6.0 km
7.0 km
8.26 km
0 m
-25 m
-50 m
-75 m
-100 m
C
C'
5x vertical exaggeration
0.5 km
1.0 km
1.5 km
2.0 km
2.5 km
3.0 km
3.5 km
4.10 km
B
Vengsøya
2x vertical exaggeration
C
azimuth
0
90
180
270
360
D
count
slope azimuth
N
Maxima 1: 21°
Maxima 2: 162°
Maxima 3: 346°

Figure 13 (previous page): Detailed illustrations of the strandflat within area 2 (see Fig. 12 for location). (**a**): Dip map covering the strandflat with onshore portions of the subarea covered by aerial photographs. Note the curved parallel ridges of the basement block adjacent to Vengsøya and Gjøssøya and bounded by larger trenches. Locations of cross-sections are given and shown below. Point of view for 3D illustration is marked. (**b**) 3D illustration of the subarea, which highlights the curved, parallel ridges. (**c**) Aspect map and (**d**) histogram showing the preferred direction of dips for slopes steeper than 5°. The preferred strikes of slopes from the aspect analysis are shown in the small circular insets (simplified rose diagrams).

Figure 14 (next page): Various detailed illustrations of the (see Fig. 12 for location). (**a**) Dip map covering the strandflat with onshore portions of the subarea covered by aerial photographs. Areas covered with aerial photographs of the sea surface indicate area where no 5x5m resolution bathymetry data is available. Note the curved ridge traceable from Sandøya and northwards before it curves around to a SSE-NNW trend. The line illustrates locations of the cross-section. Point of view for the 3D illustration is marked. (**b**) 3D illustration of the subarea, which highlights the cruved ridge northeast of Sandøya. (**c**) Aspect map and (**d**) histogram showing the preferred direction of dips for slopes steeper than 5°. Grey line shows the preferred aspects of the topography (not to scale along the Y-axis). The preferred strikes of slopes from the aspect analysis are shown in the small circular insets (simplified rose diagrams, grey lines shows topography maxima).

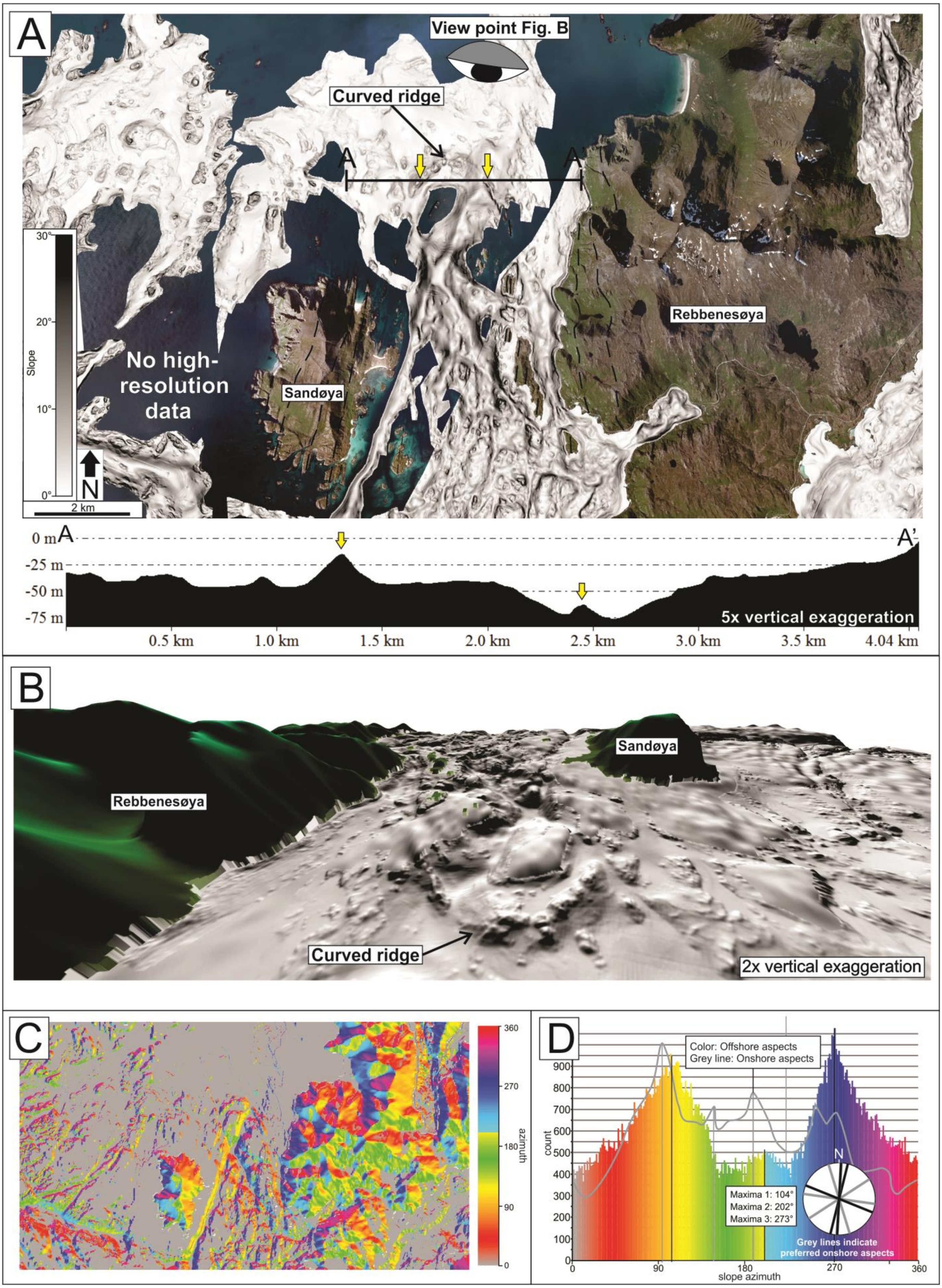
A
View point Fig. B
Curved ridge
A
A'
Slope
30°
20°
10°
0°
N
2 km
No high-resolution data
Sandøya
Rebbenesøya
0 m
-25 m
-50 m
-75 m
5x vertical exaggeration
0.5 km
1.0 km
1.5 km
2.0 km
2.5 km
3.0 km
3.5 km
4.04 km
B
Rebbenesøya
Sandøya
Curved ridge
2x vertical exaggeration
C
azimuth
360
270
180
90
0
D
Color: Offshore aspects
Grey line: Onshore aspects
count
Maxima 1: 104°
Maxima 2: 202°
Maxima 3: 273°
Grey lines indicate preferred onshore aspects
slope azimuth

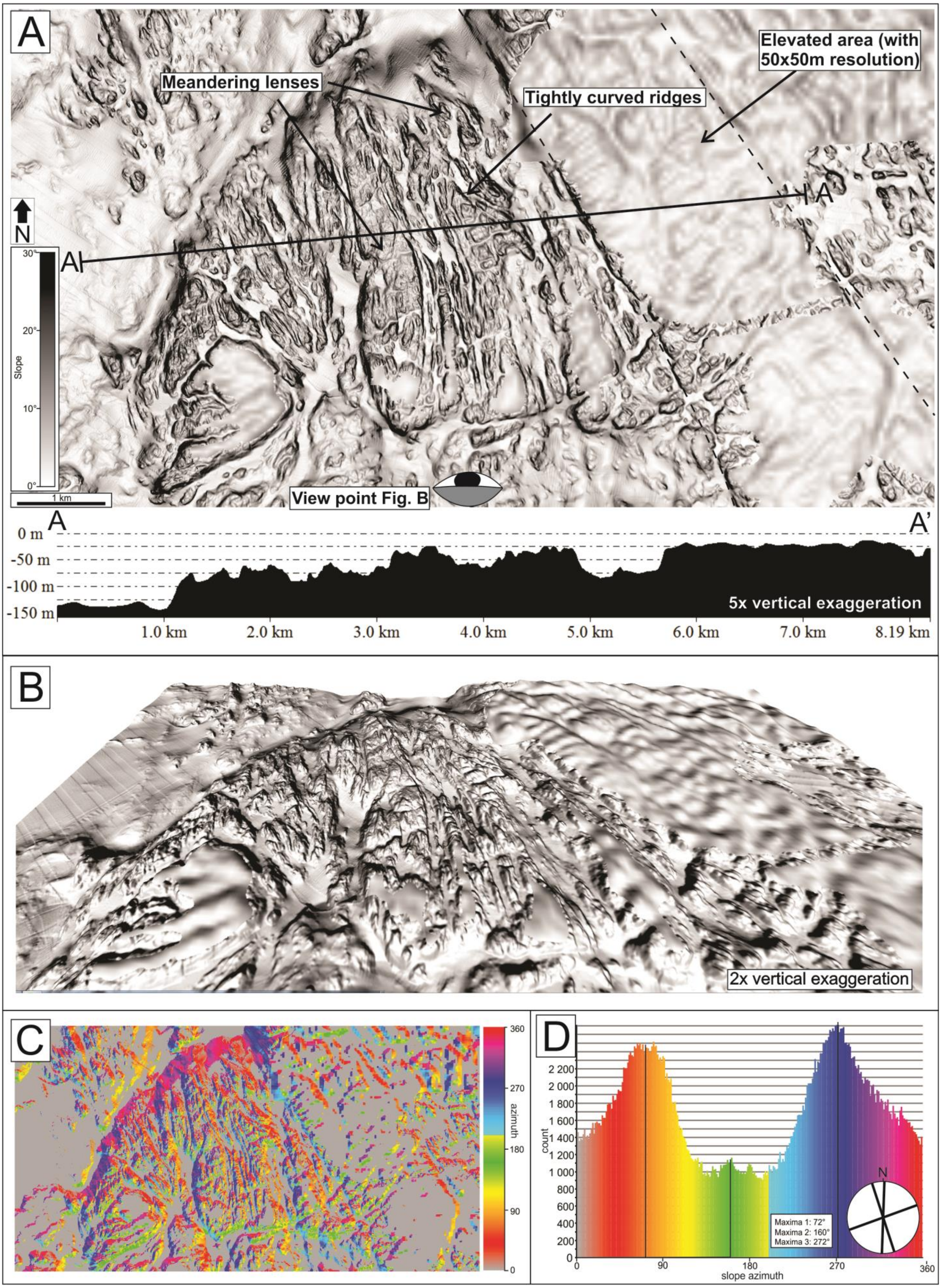
A
Meandering lenses
Tightly curved ridges
Elevated area (with 50x50m resolution)
N
Slope
30°
20°
10°
0°
1 km
A
A'
View point Fig. B
0 m
-50 m
-100 m
-150 m
5x vertical exaggeration
1.0 km
2.0 km
3.0 km
4.0 km
5.0 km
6.0 km
7.0 km
8.19 km
B
2x vertical exaggeration
C
azimuth
360
270
180
90
0
D
count
slope azimuth
Maxima 1: 72°
Maxima 2: 160°
Maxima 3: 272°
N

Figure 15 (previous page): Detailed illustrations of the strandflat within area 2 (see Fig. 12 for location). (**a**) Dip map covering the strandflat with location of cross-section given and shown below. Note the internally curved, parallel ridges and meandering lenses. Point of view for 3D illustration is marked. (**b**) 3D illustration of the subarea, which highlights the internally curved, parallel ridges. (**c**) Aspect map and (**d**) histogram showing the prefered direction of dips for slopes steeper than 5°. The preferred strikes of slopes from the aspect analysis are shown in the small circular insets (simplified rose diagrams).

Figure 16 (next page): Illustrations of the strandflat within Area 2 (see Fig. 12 for location). (**a**): Dip map covering the strandflat east of Sandøya with location of the cross-section shown below. Note the NNW-SSE trending curved, parallel ridges and the NE-SW trending trench in the southern portion of the subarea. Point of view for the 3D illustration is marked. (**b**) 3D illustration of the subarea, which highlights the curved, parallel ridges. Interpretation of the dip of a major foliation surface (ductile shear zone?) is shown. (**c**) Aspect map and (**d**) histogram showing the preferred direction of dips for slopes steeper than 5°. The preferred strikes of slopes from the aspect analysis are shown in the small circular insets (simplified rose diagrams).

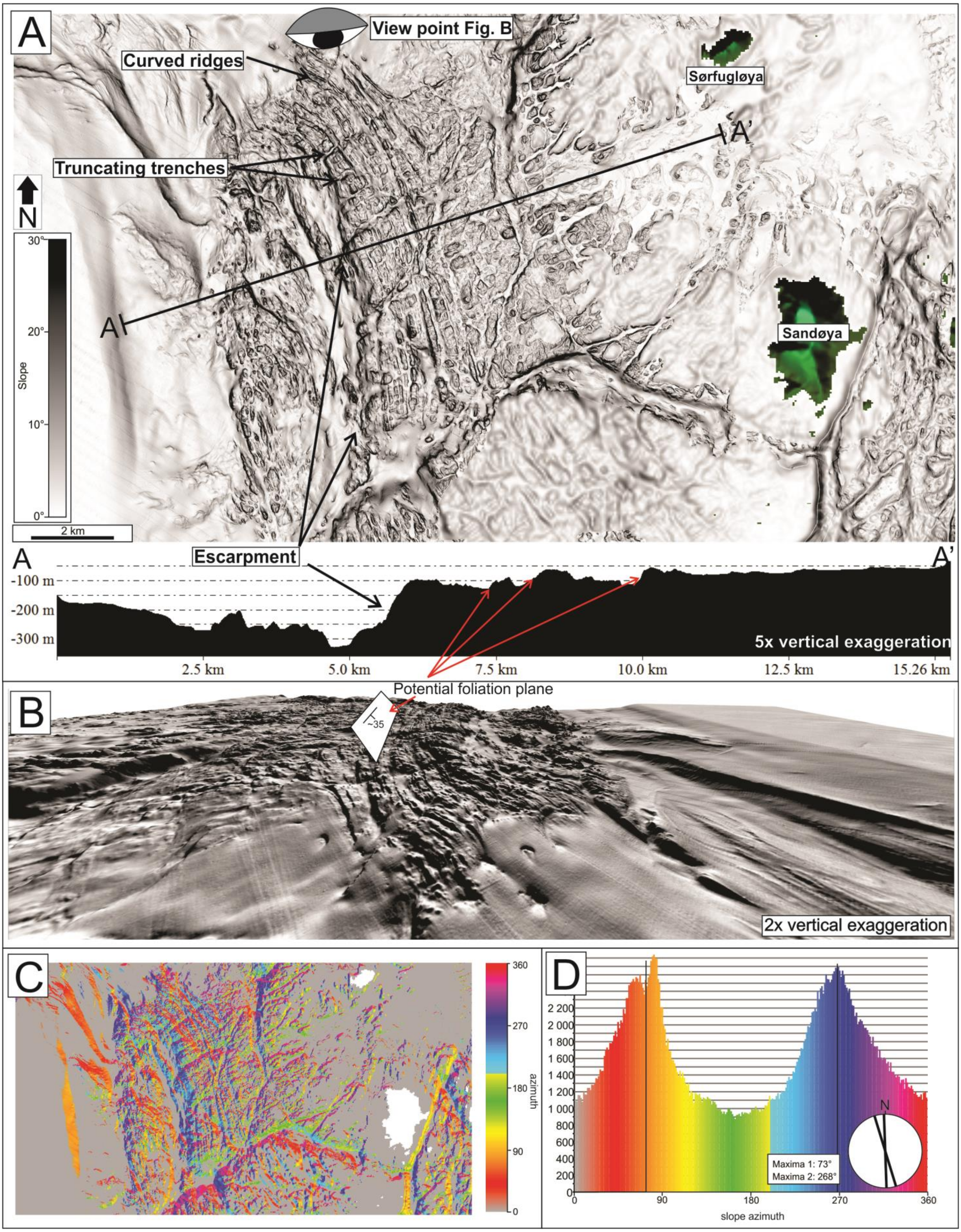
A
View point Fig. B
Curved ridges
Sørfugløya
A'
Truncating trenches
N
30°
20°
Slope
10°
0°
2 km
A
Sandøya
A
Escarpment
A'
-100 m
-200 m
-300 m
5x vertical exaggeration
2.5 km
5.0 km
7.5 km
10.0 km
12.5 km
15.26 km
Potential foliation plane
B
~35
2x vertical exaggeration
C
360
270
180
90
0
azimuth
D
2 200
2 000
1 800
1 600
1 400
1 200
1 000
800
600
400
200
0
0
90
180
270
360
slope azimuth
N
Maxima 1: 73°
Maxima 2: 268°

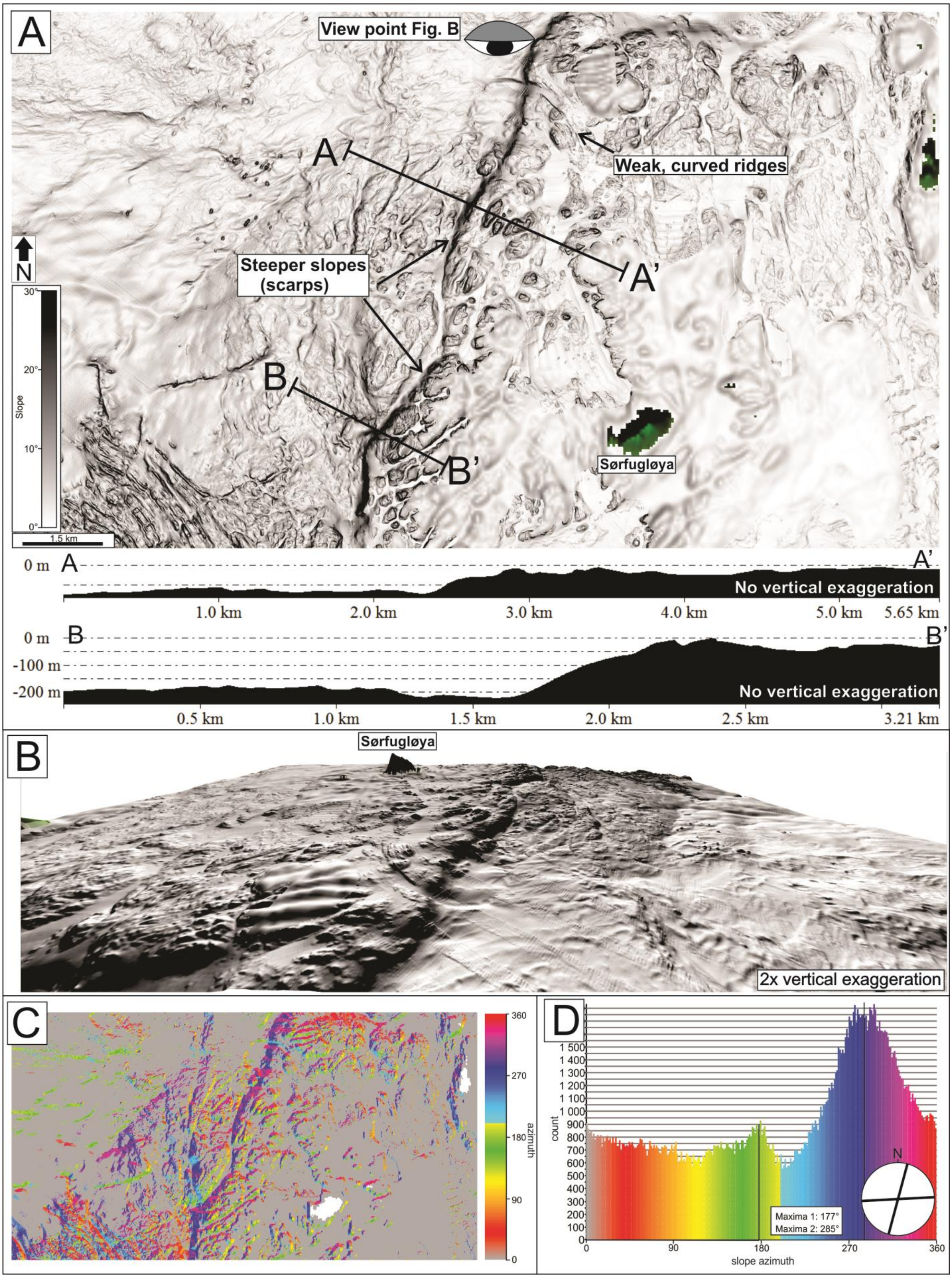

A
View point Fig. B
Weak, curved ridges
A
A'
Steeper slopes (scarps)
B
B'
Sørfugløya
N
30°
20°
10°
0°
Slope
1.5 km
0 m
A
A'
No vertical exaggeration
1.0 km
2.0 km
3.0 km
4.0 km
5.0 km
5.65 km
0 m
B
B'
-100 m
-200 m
No vertical exaggeration
0.5 km
1.0 km
1.5 km
2.0 km
2.5 km
3.21 km
B
Sørfugløya
2x vertical exaggeration
C
360
270
180
90
0
azimuth
D
count
Maxima 1: 177°
Maxima 2: 285°
N
slope azimuth

Figure 17 (previous page): Detailed illustrations of the strandflat within Area 2 (see Fig. 12 for location). (**a**) Dip map covering the strandflat northwest of Sørfugløya with location of the cross-section shown below. Note the zigzag shape of the slope trending in general NE-SW and the weak trace of curved, parallel ridges in the northern parts of the subarea. Point of view for the 3D illustration is marked. (**b**) 3D illustration of the subarea, which highlights the slope and the weak curved parallel ridges. (**c**) Aspect map and (**d**) histogram showing the preferred direction of dips for slopes steeper than 5°. The preferred strikes of slopes from the aspect analysis are shown in the small circular insets (simplified rose diagrams).

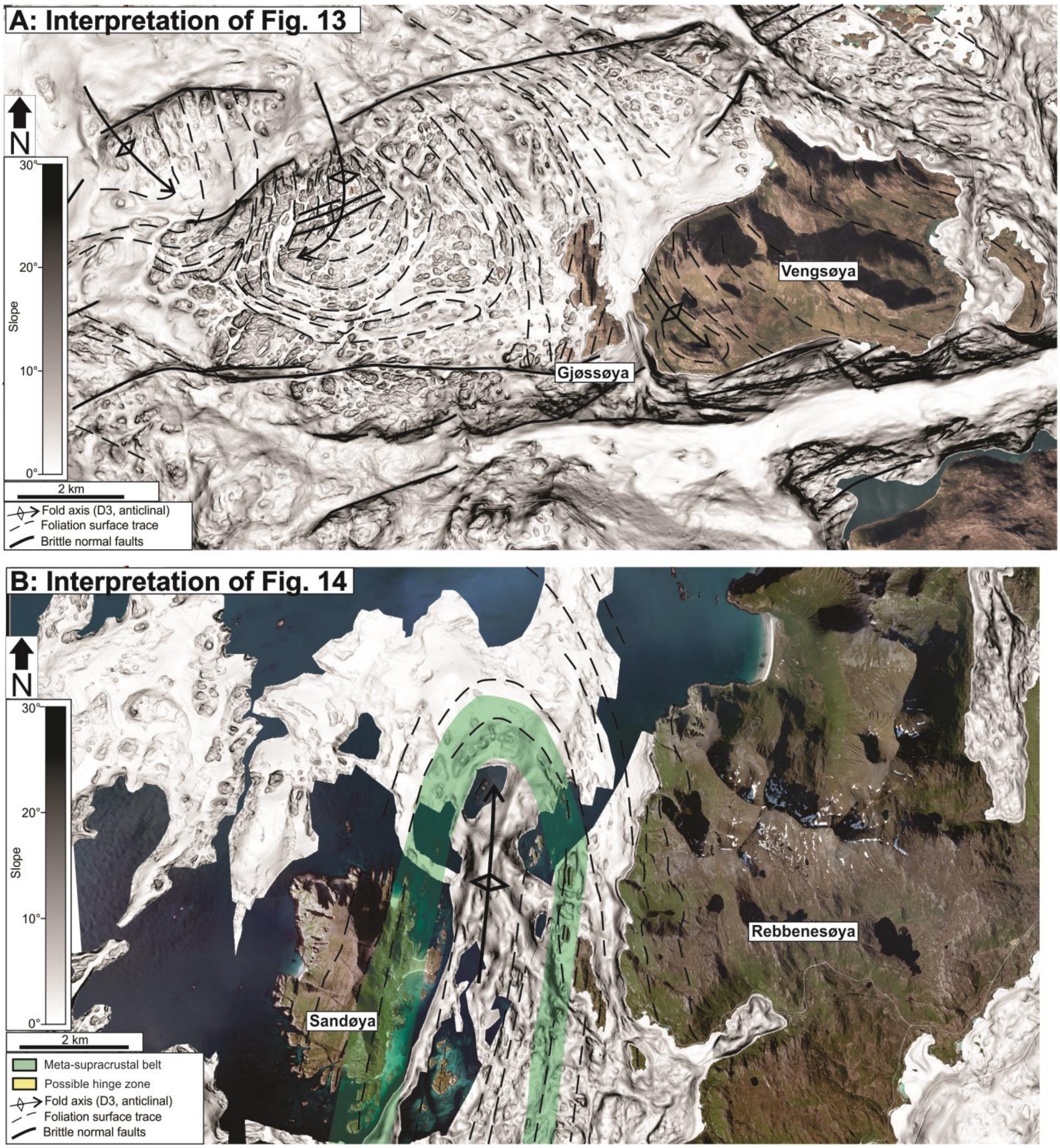

Figure 18: Interpretation of lithologies and structures present on the strandflat in Area 2 (see Fig. 12 for locations), based on correlation with known onshore structures. (**a**) The curved, parallel ridges of subarea 2.1 are interpreted as folded TTG-gneiss foliation, similar to what is observed on Vengsøya. The truncating trenches in the centre of the fold are interpreted as minor brittle faults while the larger trenches to the north and south of the fold are interpreted as major brittle faults. (**b**) The ridge tracable from Sandøya is thought to be the continuation of the quartzite unit on Sandøya. It is interpreted to be folded around a N-S trending, subvertical fold axis and may explain the opposing strikes of the foliation on Sandøya and Rebbenesøya.

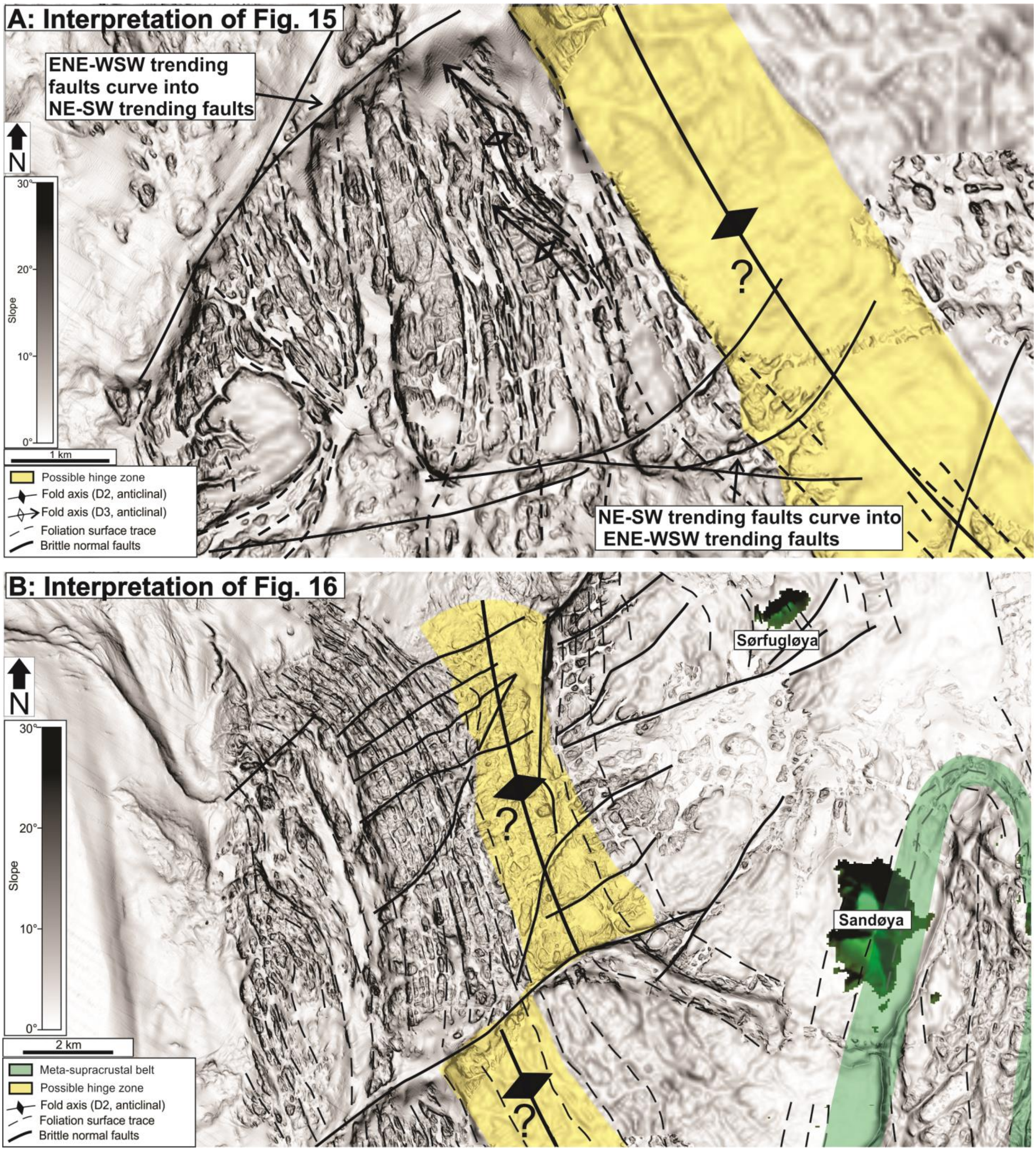

Figure 19: Interpretation of lithologies and structures covering the strandflat in Area 2 (see Fig. 12 for locations), based on correlation with known onshore structures. (**a**) The internally curved parallel ridges are interpreted as intrafolial folds that formed within a high-strain ductile shear zone. The highlighted NNW-SSE trending more diffuse area to the east is, interpreted to mark the position of either a more competent lithology, such as e.g. quartzite, or the hinge zone of an upright, sub-horizontal macro-fold. Truncating trenches are interpreted as brittle faults that bend into parallelism with each other. Note that NNE-SSW trending faults bend into parallelism with ENE-WSW trending faults in the south of the subarea, while the opposite is apparent in the northern part of the subarea. (**b**) The curved, parallel ridges are the northwards continuation of the high-strain ductile shear zone in (a). The ENE-WSW trending trench in the southern parts of the subarea is interpreted as a major brittle fault that apparently displaces the interpreted quartzite unit or macro-fold hinge-zone dextrally (yellow colour).

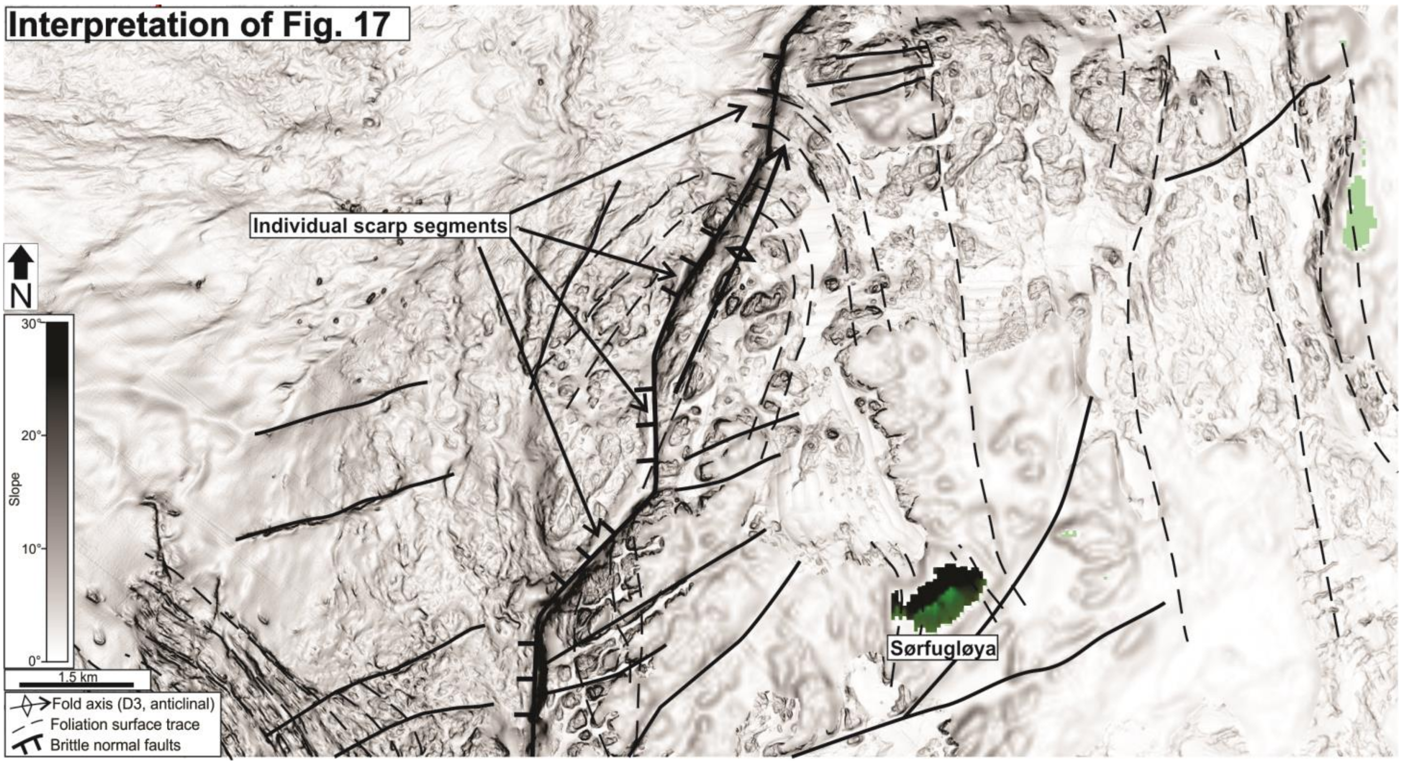

Figure 20: Interpretation of main structural features within a subarea on the strandflat in Area 2 (see Fig. 12 for location), based on correlation with known onshore structures. The zigzag-shaped slope is interpreted as an array of alternating N-S and NE-SW trending brittle normal faults that down-drop basement rocks to the west. The weak curved, parallel ridges in the northern parts of the subarea are interpreted to mark the position of a north-trending sub-vertical fold.

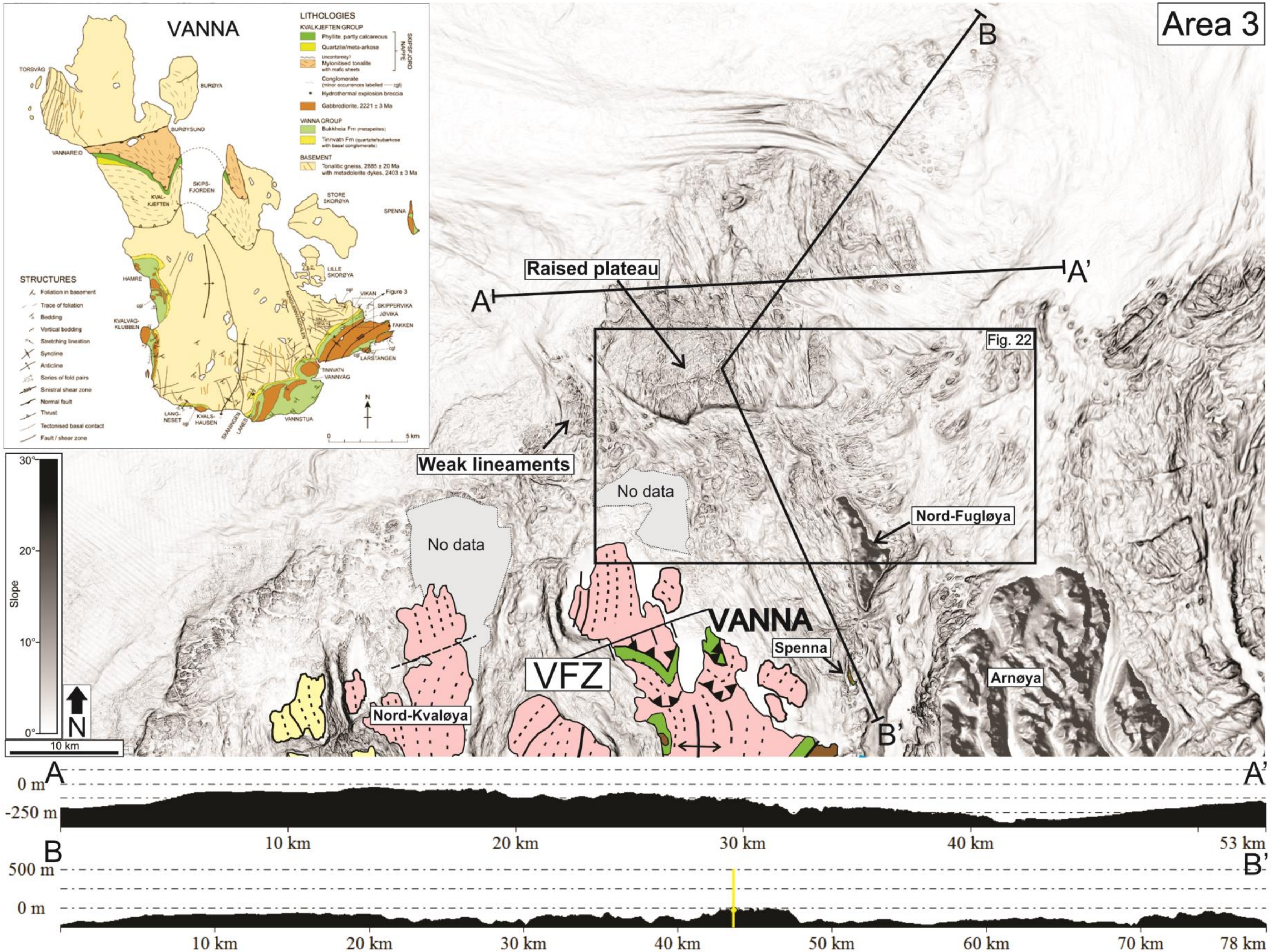

Area 3
VANNA
LITHOLOGIES
STRUCTURES
B
A
A'
Raised plateau
Fig. 22
Weak lineaments
No data
No data
Nord-Fugløya
VANNA
VFZ
Spenna
Arnøya
Nord-Kvaløya
B'
Slope
30°
20°
10°
0°
N
10 km
A
A'
0 m
-250 m
10 km
20 km
30 km
40 km
53 km
B
B'
500 m
0 m
10 km
20 km
30 km
40 km
50 km
60 km
70 km
78 km

Figure 21 (previous page): Overview of the strandflat of Area 3 north of Vanna and Nord-Fugløya, with onshore geology from Bergh et al. (2010). Location of Fig. 22 is outlined. VFZ=Vannareid-Brurøysund fault zone. **Inset map**: Geological and tectonic map of the island of Vanna. From Bergh et al. (2007b).

Figure 22 (next page): Detailed illustrations of the strandflat within Area 3 (see Fig. 21 for location). (**a**) Bathymetric dip map of the strandflat and northern parts of Nord-Fugløya. Note the prominent rise in elevation in the north, the NE-SW trending ridges northeast of Nord-Fugløya and the NW-SE trending ridges southwest of Nord-Fugløya. Location of the cross-sections are given by lines and shown below. Point of view for 3D illustration is marked. (**b**) 3D illustration of the subarea, which highlights NW-SE trending ridges to the west and north of Nord-Fugløya. (**c**) Aspect map and (**d**) histogram showing the prefered direction of dips for slopes steeper than 5°. The preferred strikes of slopes from the aspect analysis are shown in the sircular inset (simplified rose diagram).

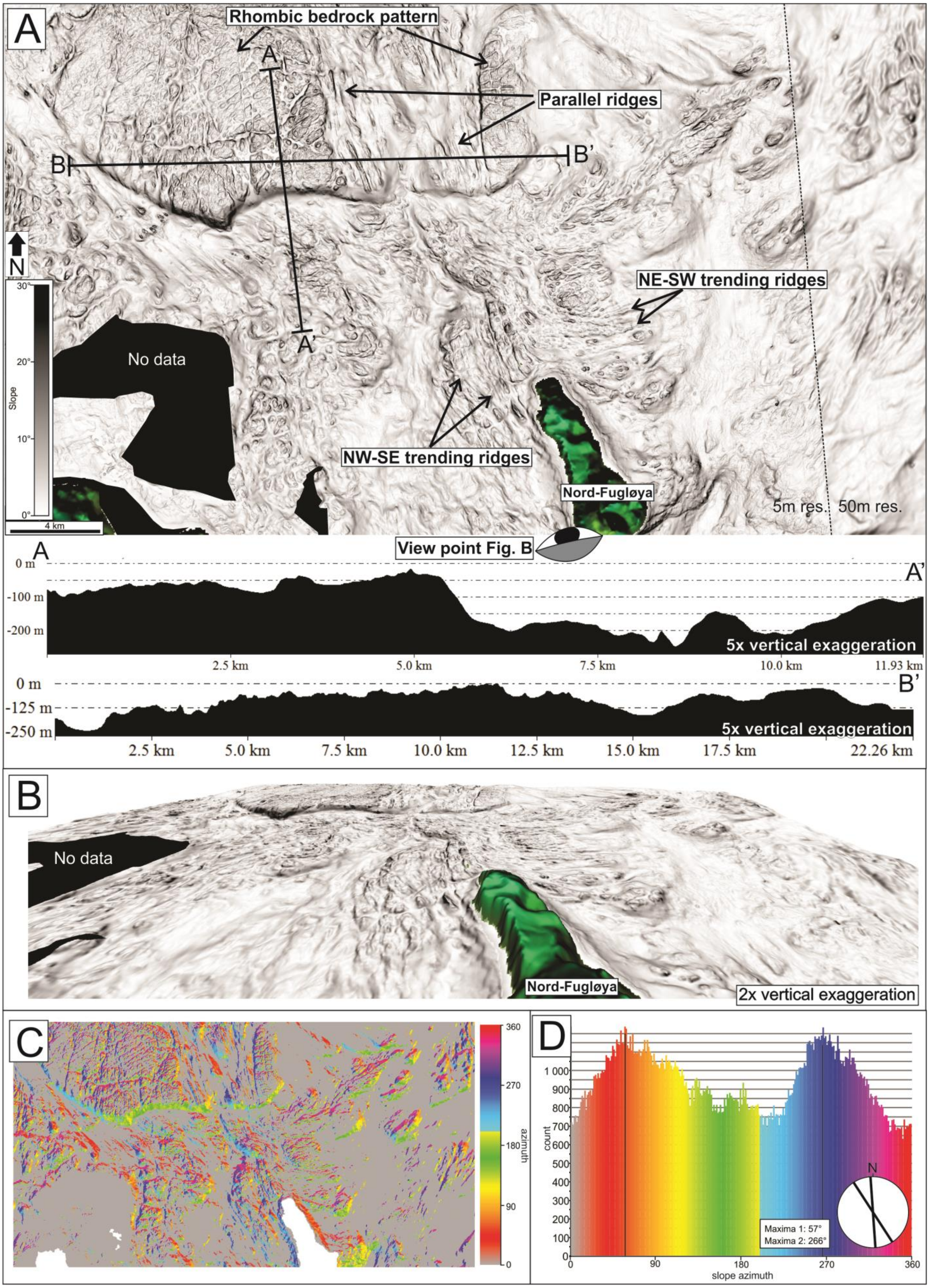
A
Rhombic bedrock pattern
Parallel ridges
B
B'
A'
N
Slope
30°
20°
10°
0°
4 km
No data
NE-SW trending ridges
NW-SE trending ridges
Nord-Fugløya
5m res.
50m res.
View point Fig. B
0 m
-100 m
-200 m
2.5 km
5.0 km
7.5 km
10.0 km
11.93 km
5x vertical exaggeration
-125 m
-250 m
12.5 km
15.0 km
17.5 km
22.26 km
2x vertical exaggeration
C
azimuth
360
270
180
90
0
D
count
slope azimuth
Maxima 1: 57°
Maxima 2: 266°

Figure 23: Detailed interpretation of the presumed WTBC – Caledonian contact and related structures covering the strandflat within Area 3 (see Fig. 21 for location), based on correlation with known onshore structures. The contact is marked by a change in the preferred orientation of NE-SW trending ridges to the northeast, relative to N-S trending ridges in the northwest, i.e. N-S trending ridges just west of Nord-Fugløya.

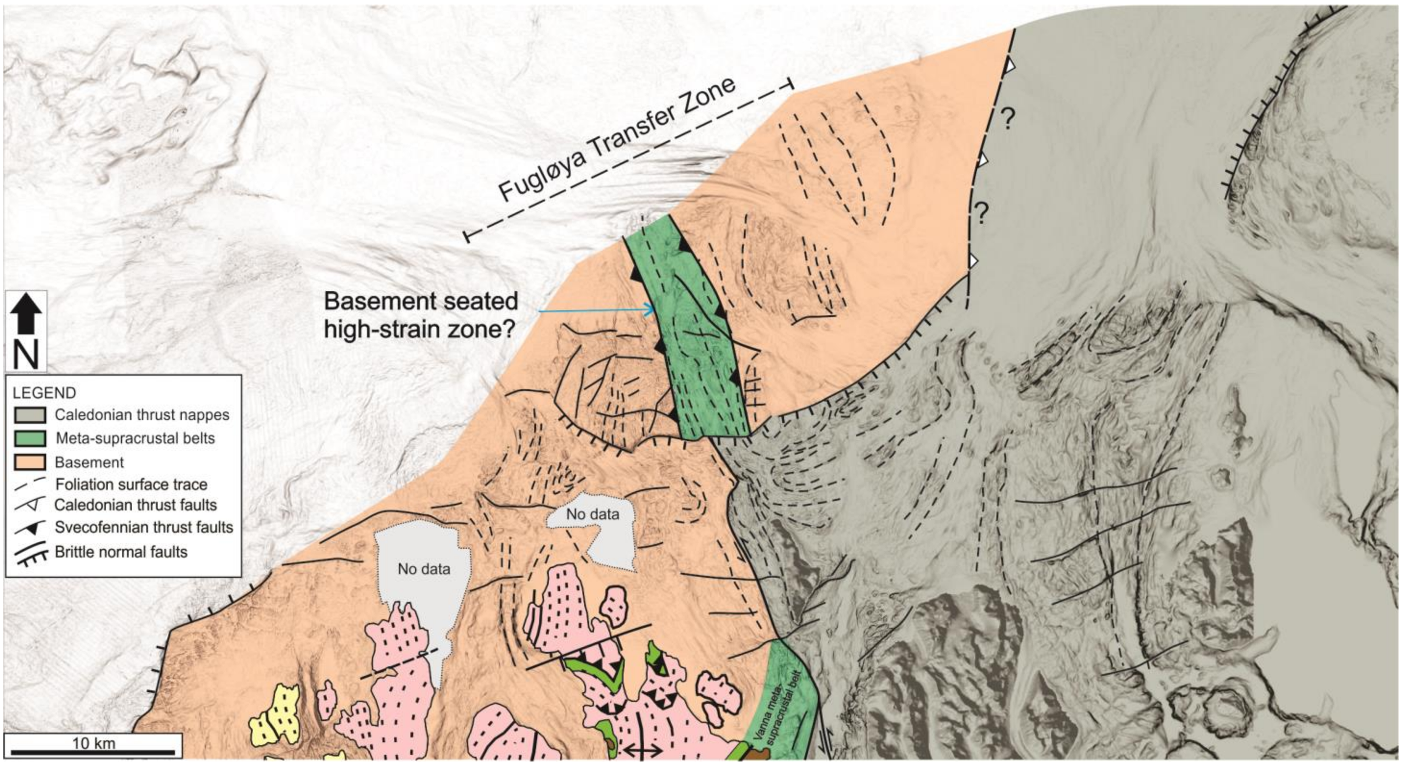

Figure 24: Interpretation of the strandflat bathymetry in Area 3, based on observation and correlation with onshore structures. The interpreted fault that defines the southern limit of the continental rise has down-faulted Caledonian nappes to the southeast, similar to what is observed along the inner portions of the WTBC. The NNW-SSE trending parallel ridges that truncate the rise are interpreted as part of a high-strain ductile zone within WTBC rocks, possibly a meta-supracrustal belt. If so, the meta-supracrustal belt, the contact towards Caledonian nappes and the Fugløya transfer zone overlap in the strait between Vanna and Nord-Fugløya.

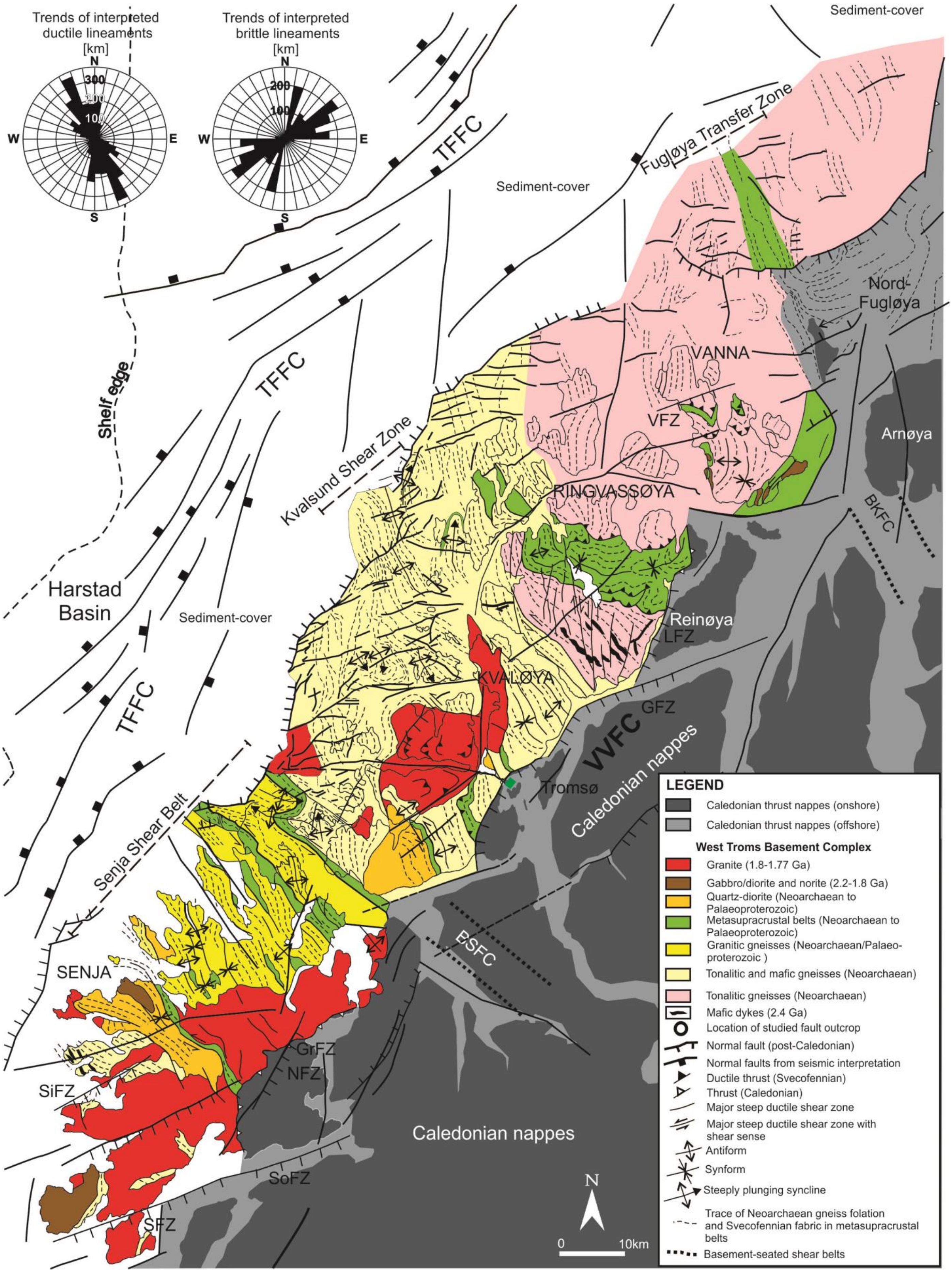
Trends of interpreted ductile lineaments [km]
Trends of interpreted brittle lineaments [km]
N
E
S
W
Sediment-cover
Fugløya Transfer Zone
TFFC
Shelf edge
Harstad Basin
Nord-Fugløya
VANNA
VFZ
Arnøya
RINGVASSØYA
Kvalsund Shear Zone
BKFC
Reinøya
LFZ
KVALØYA
GFZ
VVFC
Caledonian nappes
Tromsø
Senja Shear Belt
BSFC
SENJA
GrFZ
NFZ
SiFZ
SoFZ
SFZ
0
10km
LEGEND
Caledonian thrust nappes (onshore)
Caledonian thrust nappes (offshore)
West Troms Basement Complex
Granite (1.8-1.77 Ga)
Gabbro/diorite and norite (2.2-1.8 Ga)
Quartz-diorite (Neoarchaean to Palaeoproterozoic)
Metasupracrustal belts (Neoarchaean to Palaeoproterozoic)
Granitic gneisses (Neoarchaean/Palaeo-proterozoic)
Tonalitic and mafic gneisses (Neoarchaean)
Tonalitic gneisses (Neoarchaean)
Mafic dykes (2.4 Ga)
Location of studied fault outcrop
Normal fault (post-Caledonian)
Normal faults from seismic interpretation
Ductile thrust (Svecofennian)
Thrust (Caledonian)
Major steep ductile shear zone
Major steep ductile shear zone with shear sense
Antiform
Synform
Steeply plunging syncline
Trace of Neoarchaean gneiss folation and Svecofennian fabric in metasupracrustal belts
Basement-seated shear belts

Figure 25 (previous page): Tentative compiled bed rock and structural map of the strandflat and adjacent onshore and offshore portions of the SW Barents Sea margin, summarizing the interpretations from all areas of the strandflat by extending the onshore geology onto the strandflat. Note how the Senja Shear Belt, the Vengsøya high-strain zone and the Fugløya transfer zone segment the margin laterally. The combined length of all mapped and interpreted ductile and brittle lineaments with respect to their trends are shown in rose diagrams in the top left corner. BKFC=Bothnian-Kvænangen Fault Complex, BSFC=Bothnian-Senja Fault Complex, GFZ=Grøtsundet fault zone, GrFZ=Grasmyrskogen fault zone, LFZ=Langsundet fault zone, NFZ=Nybygda fault zone, SFZ = Stonglandseidet fault zone, SiFZ=Sifjorden fault zone, SoFZ=Solbergfjorden fault zone, VFZ=Vannareid-Brurøysund fault zone, VVFC=Vestfjorden-Vanna Fault Complex, TFFC=Troms-Finnmark Fault Complex.